

## Kinetic Modeling of Polymerization Reactions

Anil Kumar and Pankaj K. Khandelwal  
*Indian Institute of Technology—Kanpur  
 Kanpur, India*

INTRODUCTION	375
STEP GROWTH POLYMERIZATION	377
Kinetic Model of Reversible Linear Step Growth Polymerization	377
Kinetic Model for Reversible Nonlinear Step Growth Polymerization	384
RADICAL POLYMERIZATION	403
Initiation	403
Propagation Reaction	404
Termination of Polymer Radicals	405
Average Molecular Weight in Radical Polymerization	408
Gel Effect in Radical Polymerization	410
Temperature Effects in Radical Polymerization	418
REVERSIBLE RADICAL POLYMERIZATION	419
CONCLUSIONS	423
APPENDIX: ANALYTICAL SOLUTION OF ALGEBRAIC EQUATIONS	
INVOLVED IN ADDITION POLYMERIZATION	424
REFERENCES	426

### INTRODUCTION

A polymer is a high molecular weight material; polymerization is the series of reactions leading to the formation of polymers from low molecular weight material (called monomers). These can be broadly classified as step growth and chain growth polymerizations [1, 2]. In the former, the growth of molecules occurs through the reaction of reactive groups, e.g.,  $-\text{COOH}$ ,  $-\text{NH}_2$ ,  $-\text{OH}$ , located on the molecules. Polymer formation can occur through this mechanism only when the starting monomer has at least two reactive groups, when there are more than two of them in the monomer, the resultant polymer is either branched or crosslinked in structure. As opposed to this, linear polymers are formed by the polymerization of bifunctional monomers. In chain growth polymerization there are growth centers in the reaction mass, to which monomers add on successively until either all monomers are consumed or some external agent terminates the polymerization.

Depending on the nature of these growth centers, chain growth polymerization can be further classified into radical, cationic, anionic, and stereoregular polymerizations [1-8]. It has been found that different mechanisms of polymerization have different characteristics. As an example, in step growth polymerization, the weight average molecular weight of polymer formed increases with the reaction time, whereas for chain growth polymerization it reaches a certain maximum value only.

Like all other reactions in nature, polymerization is reversible. However, in almost all the studies, it is assumed to be irreversible in order to simplify the analysis. In reversible polymerization, the overall conversion is limited by equilibrium; in practice, the reverse step is suppressed by applying high vacuum and higher temperatures. Unlike reactions of low molecular weight compounds, in polymerization there is a formation of several homologs which are chemically the same but differ in their molecular weights. The reaction mass can thus be characterized by a molecular weight distribution (MWD). This is nothing but a plot of the concentration of oligomer of chain length  $n$  (denoted by  $[P_n]$ ) versus  $n$ . The different physical properties of the polymers are to a large extent dependent upon MWD and a given MWD can be equivalently represented by its moments. For polymeric systems, only the first three moments can be experimentally measured [1, 3], and they have been shown to characterize the MWD completely. The general definition of moments is given by

$$\lambda_K = \sum_{n=1}^{\infty} n^K [P_n]; \quad K = 0, 1, 2, \dots \quad (1)$$

where  $[P_n]$  is the concentration of  $P_n$  species of chain length  $n$  in the reaction mass. The number and the weight average chain lengths  $\mu_n$  and  $\mu_w$  are the polydispersity index  $\rho$  of the polymer are defined in terms of these moments as

$$\mu_n = \frac{\lambda_1}{\lambda_0} \quad (2a)$$

$$\mu_w = \frac{\lambda_2}{\lambda_1} \quad (2b)$$

$$\rho = \frac{\mu_w}{\mu_n} \quad (2c)$$

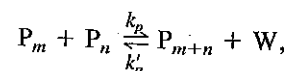
In Eq. 2c,  $\rho$  measures the breadth of the MWD and is equal to 1 for monodisperse material. On multiplying  $\mu_n$  and  $\mu_w$  with the molecular weight of the repeat unit, one obtains the number average molecular weight  $\bar{M}_n$  and the weight average molecular weight  $\bar{M}_w$ . These are known to determine the physical properties of the polymers. For example, the viscosity of molten polymers is proportional to the weight average molecular weight and above a certain value of  $\bar{M}_w$ , the viscosity usually varies [3] as  $\bar{M}_w$  [3, 4]. This is important in estimating the power requirements for pumping the reaction mass, say, through a tubular reactor, a spinnerette to obtain fibers, or extruders and molds. In another example, the aliphatic polyester formed from  $\omega$ -hydroxydecanoic acid has little strength or spinnability when  $\mu_n$  is about 25 but it gives long, extremely weak fibers that can be cold-drawn when  $\mu_n$  is about 55 [2]. However, for  $\mu_n$  above 100, it can be spun easily and cold-drawn to strong fibers. In the following section we present the analysis of batch reactors forming polymers through the reversible step growth and radical mechanisms.

## STEP GROWTH POLYMERIZATION

Step growth polymerization of a starting monomer is bifunctional and the resulting polymer is branched. The following

## Kinetic Model of Reversible Step Growth Polymerization

It is assumed that the starting monomer has two functional groups. On polymerization, the chain length, it has one unreacted functional group. The polymer can be schematically



where  $W$  is the condensation product. It is observed that polymerization is reversible in Eq. 3 and it is desired to model the reaction as a function of time. Based on the equal reactivity hypothesis, the rate of reaction is independent of the chain length of the monomers. The modeling of step growth polymerization is given by

A chemical reaction can occur between  $P_m$  and  $P_n$  and the product is  $P_{m+n}$  and  $W$ .

$$R = \alpha \omega_{m,n} Z_{m,n}$$

where  $\alpha$  is a constant of proportionality,  $\omega_{m,n}$  is the probability of reaction,  $Z_{m,n}$  is the number of reaction between two reacting species. The rate of reaction would be equal to  $sZ$ . Addition of monomers is proportional to  $[P_m]^2/2$ . Consequently, if  $k_p$  is the rate constant for the reaction, the kinetic model under

$$\begin{aligned} k_{p,mn} &= \frac{R}{[P_m][P_n]} = sk_p, \\ &= \frac{R}{[P_m]^2} = \frac{sk_p}{2}, \end{aligned}$$

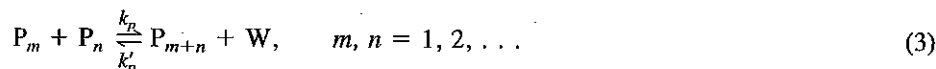
For linear chains, the reacting functional groups are  $2n$ . This means that in Eq. 5,  $s$  is a function of  $n$ . In the forward step growth polymerization, it is formed by the addition of monomers to the polymer chain.  $W$  can be removed from the reaction which would give a small total number of bonds is  $(n - 1)$ . In a batch reactor is given by

## STEP GROWTH POLYMERIZATION [1-3]

Step growth polymerization occurs through reaction of two or more reactive groups. If the starting monomer is bifunctional, the resulting polymer is linear in structure; otherwise the polymer is branched. The following analysis of batch reactors is presented for both cases.

### Kinetic Model of Reversible Linear Step Growth Polymerization

It is assumed that the starting monomer is an ARB type where A and B are the reacting functional groups. On polymerization, larger chains are formed but no matter what the chain length, it has one unreacted A and one unreacted B at its ends. The growth of the polymer can be schematically written as



where W is the condensation product and  $P_m$  is a polymer chain having  $m$  repeat units. It is observed that polymerization is represented by a set of infinite elementary reactions given in Eq. 3 and it is desired to model these kinetically to determine the MWD of the polymer as a function of time. Based on the experiments of Bhide and Sudborough, Flory proposed the equal reactivity hypothesis in which the reactivity of the reactive groups is independent of the chain length of the polymer. This serves as the most basic assumption in the modeling of step growth polymerization and is described below.

A chemical reaction can occur only when the reacting molecules collide. The rate of reaction,  $R$ , can thus be written in terms of the product of the collision frequency,  $\omega_{m,n}$ , between  $P_m$  and  $P_n$  and the probability of their reaction,  $Z_{m,n}$ . Therefore,

$$R = \alpha \omega_{m,n} Z_{m,n} \quad (4)$$

where  $\alpha$  is a constant of proportionality. From the equal reactivity hypothesis [1], the probability of reaction,  $Z_{m,n}$ , is independent of  $m$  and  $n$ . Thus, if  $Z$  is the probability of reaction between two reacting groups and  $P_m$  and  $P_n$  can react in  $s$  distinct ways,  $Z_{m,n}$  would be equal to  $sZ$ . Additionally, the collision frequency  $\omega_{m,n}$  between two dissimilar molecules is proportional to  $[P_m][P_n]$ , whereas that between  $P_m$  and  $P_n$  is proportional to  $[P_m]^2/2$ . Consequently, if  $k_p$  is the rate constant associated with the reaction of functional groups, the kinetic model under the equal reactivity hypothesis can be written as

$$k_{p,mn} = \frac{R}{[P_m][P_n]} = sk_p, \quad m \neq n; m, n = 1, 2, \dots \quad (5a)$$

$$= \frac{R}{[P_m]^2} = \frac{sk_p}{2}, \quad m = n; m = 1, 2, \dots \quad (5b)$$

For linear chains, the reacting functional groups are always located at the end of the chain. This means that in Eq. 5,  $s$  is always 2, as seen in Figure 1. Any polymer species  $P_n$  ( $n \geq 2$ ) is formed in the forward step by reacting a  $P_r$  ( $r < n$ ,  $r = 1, 2, \dots$ ) with a  $P_{n-r}$ . In the reverse reaction, it is formed by the attack of the condensation product, W, on the bonds of the polymer chain. W can react on any position of the chain but there are two locations on it which would give a small chain of the same length. For a linear polymer,  $P_n$ , the total number of bonds is  $(n - 1)$ . Consequently, the mole balance relation for  $P_n$  in a batch reactor is given by

$$\frac{d[P_1]}{dt} = 2k_p[P_1] \sum_{i=1}^{\infty} [P_i] + 2k'_p[W] \sum_{n=2}^{\infty} [P_n] \quad (6a)$$

$$\begin{aligned} \frac{d[P_n]}{dt} = & -2k_p[P_n] \sum_{m=1}^{\infty} [P_m] + k_p \sum_{r=1}^{n-1} [P_r][P_{n-r}] \\ & + 2k'_p[W] \sum_{m=n+1}^{\infty} [P_m] - k'_p(n-1)[P_n][W], \quad n \geq 2 \end{aligned} \quad (6b)$$

where  $k_p$  and  $k'_p$  are the forward and the reverse reaction rate constants, respectively. The relation for the  $k$ th moment can be derived by multiplying the preceding mole balance relations for  $P_n$  by  $n^k$  ( $k = 0, 1, 2$ ) and summing the various terms appropriately. The ultimate moment generation relations are given by [10]

$$\frac{d\lambda_0}{dt} = -k_p\lambda_0^2 + k'_p[W](\lambda_1 - \lambda_0) \quad (7a)$$

$$\frac{d\lambda_1}{dt} = 0 \quad (7b)$$

$$\frac{d\lambda_2}{dt} = 2k_p\lambda_1^2 + \frac{k'_p}{3}[W](\lambda_1 - \lambda_3) \quad (7c)$$

To be able to solve Eq. 6, the MWD of the feed to the batch reactor must be known. Let us assume that at  $t = 0$  it is given by

$$[P_n] \Big|_{t=0} = [P_n]_0, \quad n = 1, 2, 3, \dots \quad (8)$$

Correspondingly, its moments can be found and are assumed to be given by

$$\lambda_k \Big|_{t=0} = \sum_{n=1}^{\infty} n^k [P_n]_0 = \lambda_k^0, \quad k = 0, 1, 2 \quad (9)$$

Equation 7b is the easiest to integrate and it shows that the first moment  $\lambda_1$  is time invariant, equal to  $\lambda_1^0$ . It may be observed that the first moment is the same as the total count of repeat units, which is time invariant during polymerization. Equation 7c gives  $\lambda_2$  but it involves  $\lambda_3$  and can be integrated only when some information about it is known. However, if the moment generation relation for  $\lambda_3$  is written, it is found that it involves  $\lambda_4$

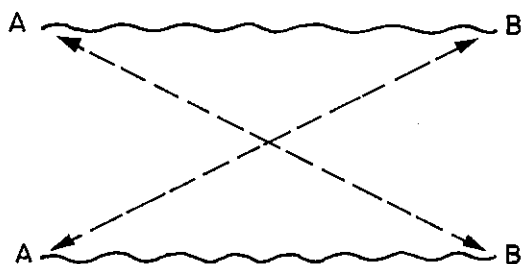


Figure 1 Schematic representation of reaction between linear chains.

and the moment generation relation has been broken by relation for the bifunctional assuming the MWD to be  $\lambda_0$ ,  $\lambda_1$ , and  $\lambda_2$  by the follow

$$\lambda_3 \cong \frac{\lambda_2(2\lambda_2\lambda_0 - \lambda_1^2)}{\lambda_1\lambda_0}$$

In the literature, computation compared with those found from been good and the approx range of computation.

The major difficulty of co the fact that the chain growth written in Eq. 6. The variou reactors are highly nonlinear solves an arbitrarily large num  $P_N$  is close to zero. However variable because higher chain like to determine the first thr concentrations of the first few entire MWD. It is possible to [18]:

$$\sum_{i=n+1}^{\infty} [P_i] = \lambda_0 - [P_n] -$$

By using Eq. 11, the MWD re

$$\frac{d[P_1]}{dt} = -2k_p[P_1] \left( \frac{\lambda_0 + k}{k_p} \right)$$

$$\begin{aligned} \frac{d[P_n]}{dt} = & -2k_p[P_n]\lambda_0 + k_p \\ & + 2k'_p[W] \left\{ \lambda_0 - \right. \end{aligned}$$

and at  $t = 0$ ;

$$[P_n] = [P_n]_0; \quad n = 1, 2, 3$$

Equations 12 are now in the dec determined sequentially by first d Eq. 7a and the problem of trunc

To illustrate the method outlin in batch reactors is analyzed w assumed that the polymer forme is governed by Raoult's law, the

$$p_r = p_r^*(T) \frac{[W]}{[W] + \lambda_0}$$

(6a)

and the moment generation relation for  $\lambda_4$  involves  $\lambda_5$ , and so on. This hierarchy of relation has been broken by using a suitable closure relation. This approximate closure relation for the bifunctional step growth polymerization was proposed in the literature by assuming the MWD to be given by the Schulz-Zimm relation for which  $\lambda_3$  is related to  $\lambda_0$ ,  $\lambda_1$ , and  $\lambda_2$  by the following relation [11, 12]:

 $n \geq 2$ 

(6b)

$$\lambda_3 \cong \frac{\lambda_2(2\lambda_2\lambda_0 - \lambda_1^2)}{\lambda_1\lambda_0} \quad (10)$$

ate constants, respectively. The  
ng the preceding mole balance  
rious terms appropriately. The

(7a)

(7b)

(7c)

1 reactor must be known. Let us

(8)

$$\sum_{i=n+1}^{\infty} [P_i] = \lambda_0 - [P_n] - \sum_{i=1}^{n-1} [P_i] \quad (11)$$

ed to be given by

(9)

$$\frac{d[P_1]}{dt} = -2k_p[P_1]\left(\frac{\lambda_0 + k'_p[W]}{k_p}\right) + 2k'_p[W]\lambda_0 \quad (12a)$$

at the first moment  $\lambda_1$  is time  
moment is the same as the total  
merization. Equation 7c gives  $\lambda_2$   
information about it is known.  
en, it is found that it involves  $\lambda_4$

$$\begin{aligned} \frac{d[P_n]}{dt} = & -2k_p[P_n]\lambda_0 + k_p \sum_{r=1}^{n-1} [P_r][P_{n-r}] - 2k'_p[P_n][W](n+1) \\ & + 2k'_p[W]\left\{\lambda_0 - \sum_{i=1}^{n-1} [P_i]\right\}, \quad n \geq 2 \end{aligned} \quad (12b)$$

and at  $t = 0$ ;

$$[P_n] = [P_n]_0; \quad n = 1, 2, 3, \dots \quad (12c)$$

Equations 12 are now in the decoupled form and the concentration of any species can be determined sequentially by first determining the zeroth moment of distribution,  $\lambda_0$ , through Eq. 7a and the problem of truncation error is completely eliminated.

To illustrate the method outlined above, formation of polyethylene terephthalate (PET) in batch reactors is analyzed with ethylene glycol (EG) evaporating [19-21]. If it is assumed that the polymer formed cannot be evaporated and the vapor-liquid equilibrium is governed by Raoult's law, then

$$p_r = p_r^*(T) \frac{[W]}{[W] + \lambda_0} \quad (13)$$

chains.

where  $p_r$  and  $p_p^*(T)$  are the pressure applied on the reactor and the vapor pressure of the condensation product and  $[W]$  is the concentration of the condensation product. Experiments have shown that PET has an equilibrium constant  $K(=k_p/k'_p)$  of 0.5, which is independent of temperature, and conversion of 99% is needed to obtain fiber-grade polymer. In order to push the polymerization in the forward direction, high vacuum and temperature are applied. The effect of the polymerization pressure and the temperature can be evaluated through the use of Eqs. 7, 12, and 13 as follows. To obtain the solution of Eqs. 12 and 13, they are written in the nondimensional form using the following variables [18]:

$$P_n = \frac{[P_n]}{\lambda_1^0} \quad (14a)$$

$$\beta = \frac{k'_p}{k_p} \equiv \frac{1}{K} \quad (14b)$$

$$t' = k_p \lambda_1^0 t \quad (14c)$$

$$w = \frac{[W]}{\lambda_1^0} \quad (14d)$$

where

$$\lambda_1^0 = \sum_{n=1}^{\infty} n[P_n]_0 \quad (14e)$$

It is assumed that the feed to the batch reactor has its MWD given by Flory's distribution with conversion  $p_A$  of functional groups as 0.3; i.e., at  $t = 0$ ,

$$p_n = (1 - 0.3)(0.3)^n$$

The moment equations can be derived; they are

$$\frac{d\lambda_0}{dt} = -\lambda_0^2 + \beta W(\lambda_1 - \lambda_0) \quad (15a)$$

$$\frac{d\lambda_1}{dt} = 0 \quad (15b)$$

$$\frac{d\lambda_2}{dt} = 2\lambda_1^2 + \frac{\beta}{3} W(\lambda_1 - \lambda_3) \quad (15c)$$

These can be solved using the closure relation given in Eq. 10. Once the pressure and the temperature are specified,  $\lambda_0$ ,  $\lambda_2$ ,  $P_1$ , and  $P_2$  can be found from Eqs. 15 and 16 using the Runge-Kutta numerical technique. The concentration of the condensation product  $W$  is obtained from Eq. 13 assuming the escaping vapors and the liquid are in thermodynamic equilibrium.

By using the computation method outlined here, it is possible to determine  $\lambda_0$ ,  $\lambda_2$ ,  $P_1$ , and  $P_2$  as a function of the dimensionless reaction time and the  $\mu_n$  and  $\rho$  are computed using Eq. 2. At low pressures, a large amount of EG is evaporated and  $\mu_n$  and  $\rho$  increase continuously with time (as shown in Fig. 2). This implies that the polymers formed at low reaction pressures are highly polydispersed long-chain species. As opposed to this, at high pressures, the situation is found to be just the opposite. The dimensionless concentrations of the first two species  $P_1$  and  $P_2$  are presented in Figure 3 at different system pressures.

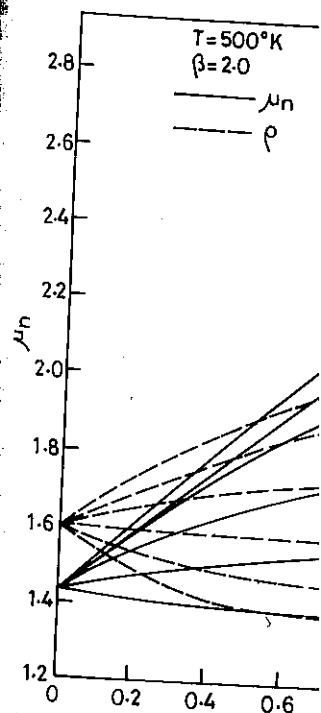


Figure 2 Number average chain values of reaction pressures ( $T = 500^\circ\text{K}$ ,  $\beta = 2.0$ ).

As the reaction proceeds the consumption of the monomer decreases, thus reducing the reaction time. The reactor pressure affects the concentration of the dimer,  $P_2$ , which is specified at equilibrium point. We thus see from Figure 3 that the equilibrium point is delayed.

When the temperature of the reaction is increased, the reaction time is reduced, thus reducing the reaction time. In step growth polymerization, the reaction time is unaffected by the temperature. For different temperatures, the chain length species are formed at different times. The effect of higher temperature is significant when the equilibrium is delayed.

In the analysis presented above, it is assumed that all oligomers have the same reactivity, regardless of the number of functional groups they are located on. The comparison of the calculated reactivity with experimental data has

the vapor pressure of the  
ensation product. Experi-  
=  $k_p/k'_p$ ) of 0.5, which is  
led to obtain fiber-grade  
rection, high vacuum and  
ssure and the temperature  
ws. To obtain the solution  
form using the following

(14a)

(14b)

(14c)

(14d)

(14e)

ven by Flory's distribution

(15a)

(15b)

(15c)

. Once the pressure and the  
m Eqs. 15 and 16 using the  
condensation product W is  
liquid are in thermodynamic

ble to determine  $\lambda_0, \lambda_2, P_1$ ,  
the  $\mu_n$  and  $\rho$  are computed  
rated and  $\mu_n$  and  $\rho$  increase  
the polymers formed at low  
. As opposed to this, at high  
imensionless concentrations  
different system pressures.

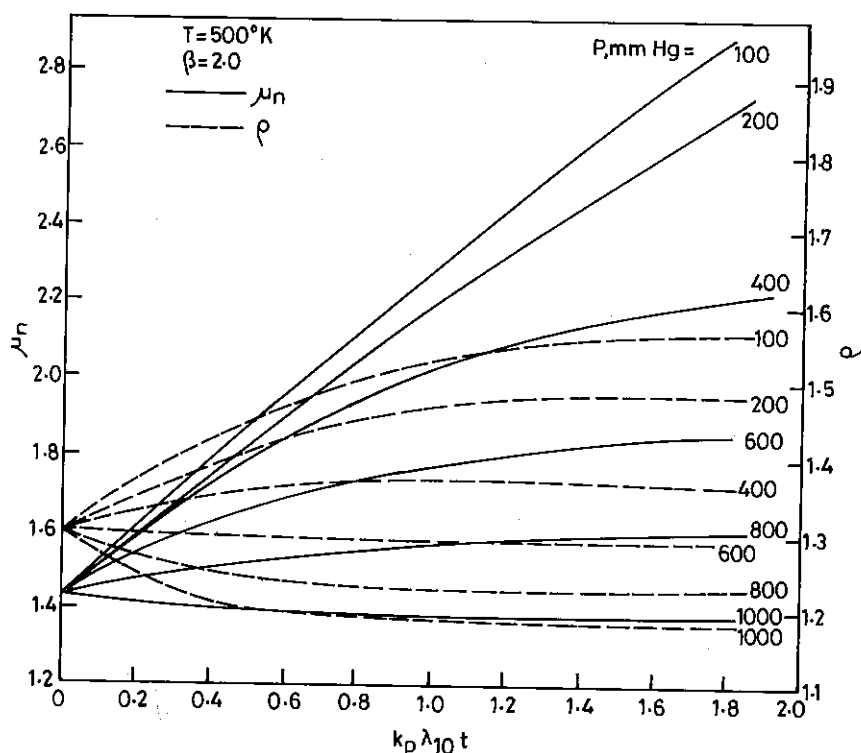


Figure 2 Number average chain length,  $\mu_n$ , and polydispersity index,  $\rho$ , versus time, for various values of reaction pressures ( $T = 500$  K,  $\beta = 2.0$ ).

As the reaction proceeds the monomer,  $P_1$ , converts into the higher oligomers. The consumption of the monomer depends on the extent of the forward reaction. It is thus seen that the reactor pressure affects the consumption of  $P_1$  in the reaction mass. Similarly, the concentration of the dimer,  $P_2$ , increases with the residence time of the reactor. The equilibrium point is specified when the concentration of any species does not change with time. We thus see from Figure 3 that the equilibrium is delayed as the system's pressure is reduced.

When the temperature of the reactor is increased, the vapor pressure  $p^*$  in Eq. 13 goes up, thus reducing the reaction mass. This in turn reduces the effect of the reverse step in step growth polymerization. In PET reactors, it is seen that the equilibrium constant,  $K$ , is unaffected by the temperature. Figures 4 and 5 present data for  $P_1, P_2, \mu_n$ , and  $\rho$  with the reaction times for different temperatures. It is found that at high temperatures, higher chain length species are formed and the polymer mass is also highly polydispersed. The effect of higher temperature is similar to that of the reduction of the total pressure and the equilibrium is delayed.

In the analysis presented above, it was assumed that the functional groups of various oligomers have the same reactivity, independent of the chain length,  $n$ , of the molecules they are located on. The comparison of computed results with the assumption of equal reactivity with experimental data has sufficiently indicated that the overall polymerization

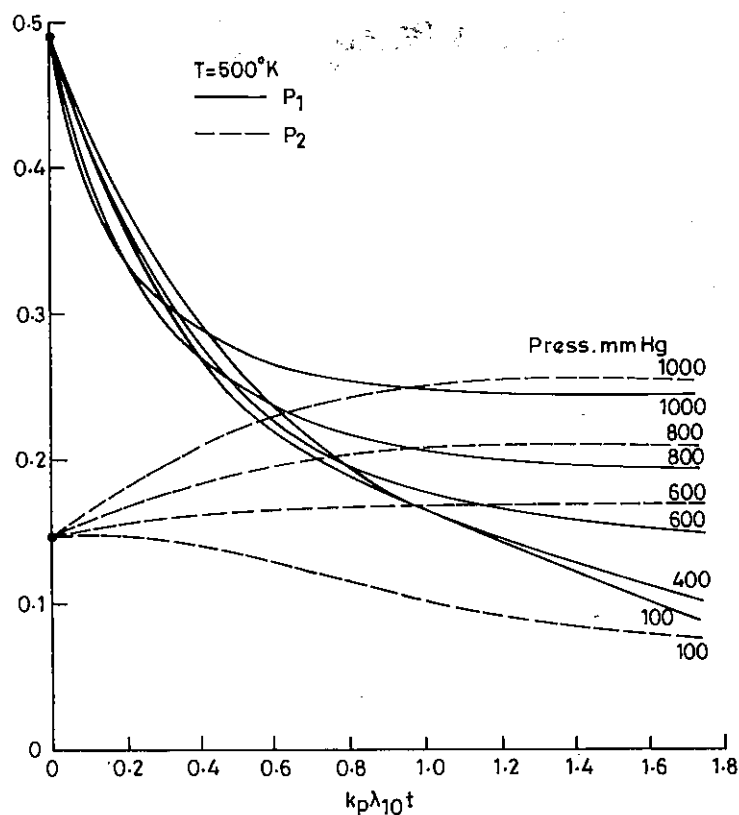


Figure 3 Effect of reactor pressure on concentrations of  $P_1$  and  $P_2$ .  $P_{10} = 0.49$ ,  $P_{20} = 0.143$ .

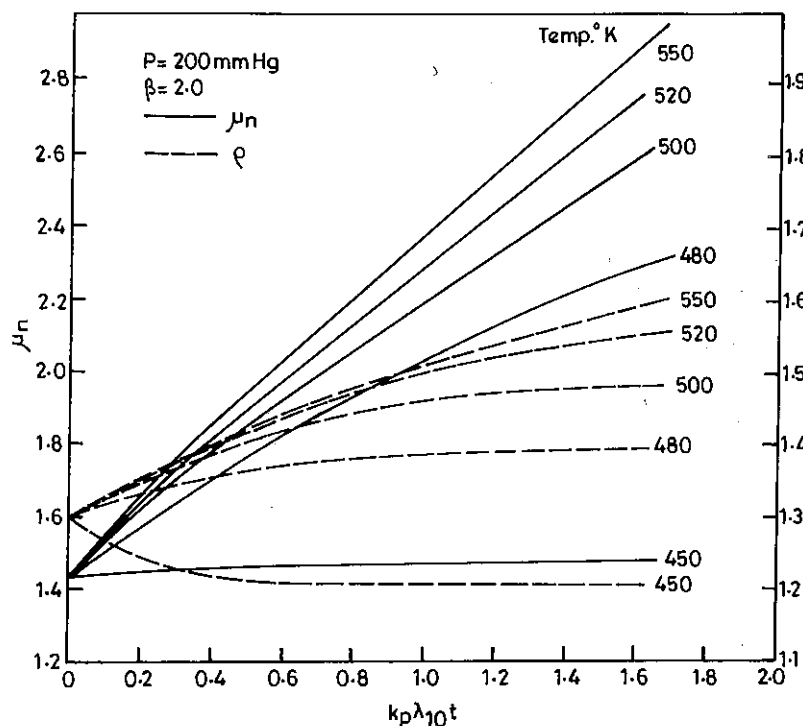


Figure 4 Number average chain length,  $\mu_n$ , and polydispersity index,  $\rho$ , versus time,  $t$ , for various values of reaction temperatures ( $P = 200$  mm Hg,  $\beta = 2.0$ ).

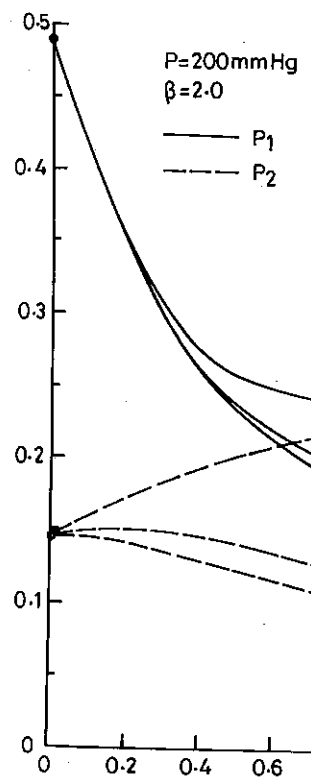
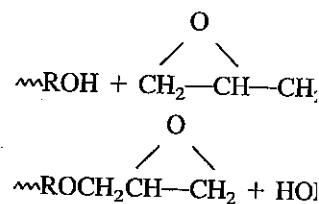


Figure 5 Effect of reactor temperature on concentrations of  $P_1$  and  $P_2$ .

is far more complex and the as [22]. In addition, as the poly increases several fold and the used, becomes mass transfer c

In the reaction-controlled re observed. This can arise when polymerization of a diacid with have different reactivities. Th bologically as the polymerization C react with A with different anhydrides, generates two func cess and these two steps gene resins can be represented by the





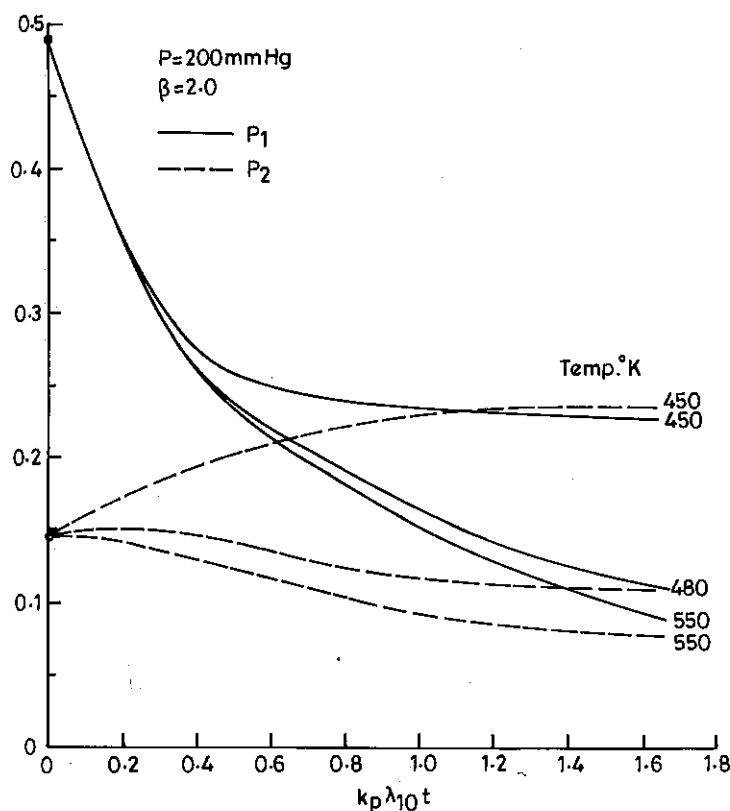
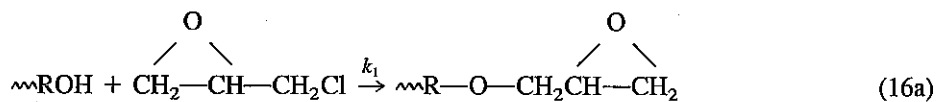


Figure 5 Effect of reactor temperature on concentration of  $P_1$  and  $P_2$ .

is far more complex and the assumption of equal reactivity is a considerable simplification [22]. In addition, as the polymerization progresses, the viscosity of the reaction mass increases several fold and the overall reaction, at some stage depending on the reactor used, becomes mass transfer controlled [13, 23–25].

In the reaction-controlled region, unequal reactivity of functional groups is commonly observed. This can arise when the reacting groups are not kinetically equivalent, as in the polymerization of a diacid with a glycol having primary and secondary OH groups which have different reactivities. These asymmetric monomers are usually represented symbolically as the polymerization of (AA + BC) monomers where functional groups B and C react with A with different rate constants. The ring-opening reaction, as found in anhydrides, generates two functional groups which participate in the chain-building process and these two steps generally have different reactivities. The formation of epoxy resins can be represented by the following equations:



000  
000  
800  
800  
600  
600  
400  
100

1.8

$P_{10} = 0.49, P_{20} = 0.143$ .

550  
520  
500  
480  
550  
520  
500  
480  
450  
450  
1.8 2.0

index,  $\rho$ , versus time,  $t$ , for

where  $k_1$  and  $k_2$  are the different rate constant values. In urethane polymerization, the unequal reactivity is explained by examining the effect of charge densities of the isocyanate groups on the phenyl diisocyanate monomer,  $\text{OCN}-\text{C}_6\text{H}_4-\text{NCO}$ . As one of the isocyanate group reacts, the positive charge on the phenyl group reduces from its initial value and the reactivity of the second  $-\text{NCO}$  group falls. This phenomenon is known as induced asymmetry and can be modeled kinetically as



where AA represents the diisocyanate. Case analyzed various situations of asymmetry and induced asymmetry and derived the molecular weight distribution in terms of the probabilities of reaction of the various functional groups [26].

There is another class of unequal reactivity polymerization in which the rate constants of the various oligomers are dependent on their chain lengths. This is chain length dependent reactivity [16, 27–36], which is found, for example, in the polymerization of sodium-*p*-fluorothiophenoxide [37]. In this, the reaction mass has more unreacted monomer than that predicted by the equal reactivity hypothesis. This observation suggests that the monomer has a lower reactivity. In the formation of polyamides, on the other hand, polymer molecules are found to have lower reactivity [38].

### Kinetic Model for Reversible Nonlinear Step Growth Polymerization

Nonlinear step growth polymerization takes place with monomers  $\text{RY}_f$  having functionality,  $f > 2$ . In this Y is the reactive group which on reaction gives rise to chemical bonds. There are several industrially important nonlinear step growth polymerization systems and some of these are polyesters from adipic acid or phthalic anhydride and glycerol or pentaerythritol (alkyl resins), curing of epoxy propolymers with diamines, curing of phenol formaldehyde polymers with hexamethylene tetramine, etc. In this class of polymerization, branched molecules are formed at low conversions of reactive groups. At a well-defined conversion  $[= 1/(f-1)]$ , some of these branched molecules are found to combine into an infinite network structure of macroscopic dimensions, called a gel [1]. This phenomenon occurs long before the reactive groups are completely consumed, and the point at which this occurs is referred to as the critical or gel point. Experimentally, the gel point is recognized as the state when the viscosity of the reaction mass becomes infinite and "gas bubbles" fail to rise through the reaction mass.

The study of nonlinear step growth polymerization is more complex than that of the linear case, and several approaches have been taken by different workers in this area to model the nonlinear. Flory [1, 39, 40] and Stockmayer [41–44] have approached this problem by determining the probabilities of finding various branched molecular structures in the reaction mass. Thereafter, they used these probability distributions to compute the number and weight average molecular weights of the polymer before gelation. Their approach, however, becomes exceedingly complex for systems of industrial importance. Other workers [45–47] have attempted to derive the average molecular weights directly, without first obtaining the detailed distributions. However, the kinetic approach presented in this section is more advantageous than the other approaches because it can be used easily to predict the behavior of nonlinear polymerization in homogeneous continuous

stirred tank reactors (HC intramolecular reactions).

The analysis using the with Y functional group represents an  $n$ -mer in the  $nf - 2(n - 1)$  unreacted reaction of two Y group analysis has been made for monomer of functionality functional groups of different. When the reactive groups modeling of the intramolecular research [58–70]. Jacobson lar bonds and observed that within a small volume,  $V_s$ , only a crude description of theory of chain statistics to presence of bond angle restrictions the cyclization constraints that they are parallel to each other.

The reverse step to this is molecules of the condensate mer chains are in general linear reaction becomes considerable because when W reacts with small chains. Let us now Regardless of its structure, it two equivalent sites on it will Fig. 6a). It is thus seen that lower molecular weight out linear polymers. However, reverse step is found to be 6b,  $P_{10}$  is assumed to be of figure it is seen that a star equivalent sites where, by the  $P_{14}$ ,  $P_{15}$ , and  $P_{16}$  can be formed one branch at a given branch equal number of repeat units the molecule has a total of  $r$  repeat where  $P_n$  will be formed on number of sites on  $P_r$  that would term accounts for the structure  $n$ . If in Figure 6c,  $P_r$  has  $b$  branches found that

$$\begin{aligned} \delta_{r \rightarrow i} &= \delta_{r \rightarrow (r-i)} = b + 2 \\ \delta_{r \rightarrow i} &= 0 \end{aligned} \quad \left. \begin{aligned} & \\ &= 2 \end{aligned} \right\}$$

where  $m = 1, 2, \dots$



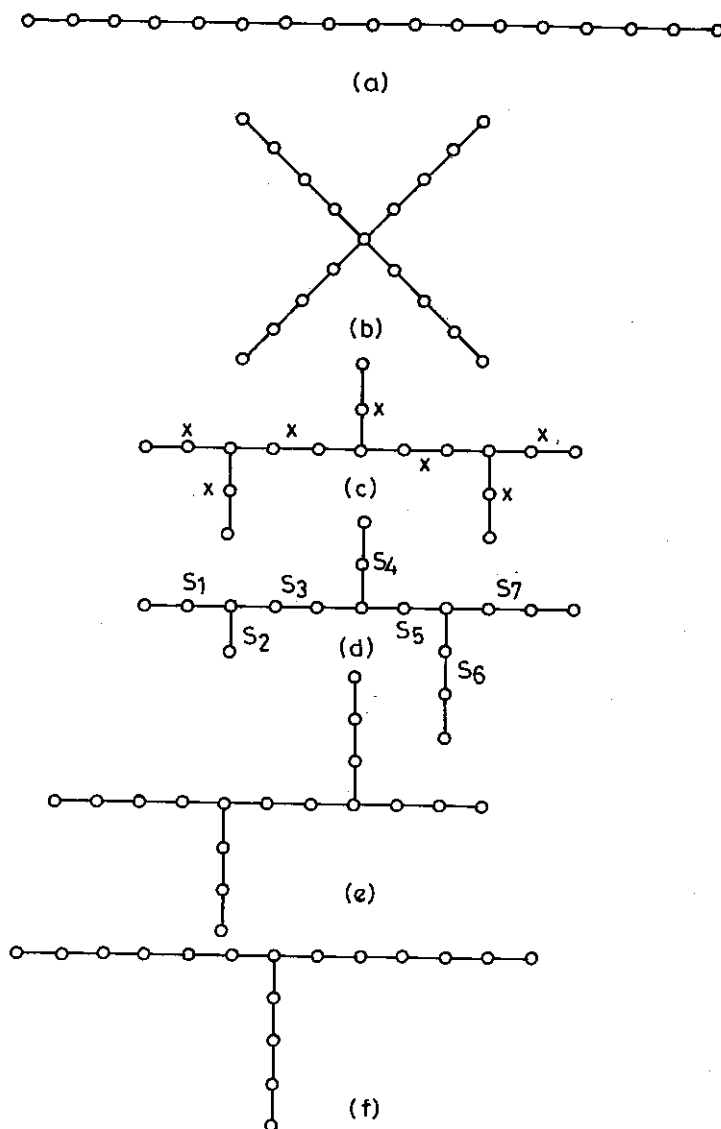


Figure 6 Structures of branched polymer chains.

The structure shown in Figure 6c can be further generalized by assuming unequal lengths of the segments. For any general chain structure, to find  $\delta_{r \rightarrow n}$ , the (a) location, number, and lengths of various branches and (b) chain length of the molecule must be known. It is then possible to work out the length of the backbone and determine  $\delta_{r \rightarrow n}$  using a computer program as follows.

We first characterize any branched molecule by dividing it into different segments in Figure 6d where the molecule is divided into seven segments  $s_1$  to  $s_7$ . If each branch is

treated as one of the segments. The total number of segments

$$n_s = 2b + 1$$

Since the segments lengths are  $n_B$ , and the location of branches

$$n_B = r - \sum_{i=1}^b s_{2i}$$

$$K_m = K_{m-1} + s_{2m-1}$$

For example, in Figure 6a, this case backbone chain length is 11 and 8 on the backbone.

To find  $\delta_{r \rightarrow n}$ , backbone segments are defined. These specify the  $q$ th positions from the forward and reverse ends. Figure 6d, if the chain is scanned from this end, and this, in the reverse direction, index  $I_4 = 7$ . For symmetry, otherwise they are not. The information so generated is used to avoid the counting of both ends up to its midpoint.

$$N_{1/2} = \frac{r}{2}, \quad r \text{ even}$$

$$= \frac{r-1}{2}, \quad r \text{ odd}$$

It is evident that the number of segments  $P_{r \rightarrow n}$  out of  $P_r$  is equal and

$$\delta_{r \rightarrow n} = \delta_{r \rightarrow (r-n)}$$

The algorithm presented for scanning branches are scanned to find the forward and reverse directions generated from various chain segments.

For all branched molecules:

$$\sum_{n=1}^{r-1} \delta_{r \rightarrow n} = 2(r-1)$$

$$\sum_{n=1}^{r-1} n \delta_{r \rightarrow n} = r(r-1)$$

treated as one of the segments, it is then observed that every alternate segment is a branch. The total number of segments,  $n_s$ , and the number of branches,  $b$ , are related by

$$n_s = 2b + 1 \quad (19)$$

Since the segments lengths  $s_i$  ( $i = 1, 2, \dots, n_s$ ) are known, the backbone chain length,  $n_B$ , and the location of branch points  $K_m$  ( $m = 1, 2, \dots, b$ ) in  $P_r$  are related by

$$n_B = r - \sum_{i=1}^b s_{2i} \quad (20a)$$

$$K_m = K_{m-1} + s_{2m-1} + 1, \quad K_0 = 0 \quad (20b)$$

$$m = 1, 2, \dots, b$$

For example, in Figure 6d,  $s_1 = 2$ ,  $s_2 = 1$ ,  $s_3 = 2$ ,  $s_4 = 2$ ,  $s_5 = 1$ ,  $s_6 = 3$ , and  $s_7 = 3$ . For this case backbone chain length  $n_B$  is 11 and branch point locations  $K_m$  are positions 3, 6, and 8 on the backbone.

To find  $\delta_{r \rightarrow n}$ , backbone indices  $I_p$  and  $I'_q$  for the forward and the reverse directions are defined. These specify the number of repeat units if the backbone is broken at the  $p$ th and  $q$ th positions from the forward and reverse directions respectively. As an example, in Figure 6d, if the chain scission occurs at the seventh bond of the backbone, molecule  $P_{10}$  is formed from this end, and which gives  $I_7 = 10$  in the forward direction. As opposed to this, in the reverse direction, the same bond breakage gives  $P_7$  and the corresponding index  $I'_4 = 7$ . For symmetric chains, the values of  $I_p$  and  $I'_q$  for same  $p$  and  $q$  are identical; otherwise they are not. The flow chart for generating these indices is given in Table 1. The information so generated is used to find  $\delta_{r \rightarrow n}$ ; the algorithm for this is given in Table 2. To avoid the counting of the available sites twice, scanning of the molecule is done from both ends up to its midpoint,  $N_{1/2}$  given by

$$N_{1/2} = \frac{r}{2}, \quad r \text{ even}$$

$$= \frac{r-1}{2}, \quad r \text{ odd} \quad (21)$$

It is evident that the number of possible sites for forming  $P_n$  ( $n = 1, 2, \dots, r-1$ ) and  $P_{r-n}$  out of  $P_r$  is equal and

$$\delta_{r \rightarrow n} = \delta_{r \rightarrow (r-n)} \quad (22)$$

The algorithm presented in Table 2 is divided into two major sections. In the first, branches are scanned to find  $\delta_{r \rightarrow n}$ . In the second, scanning of the backbone is done from the forward and reverse directions. Results for  $\delta_{17 \rightarrow n}$  ( $n = 1, 2, \dots, 16$ ) have been generated from various chain structures seen in Figure 6 and summarized in Table 3.

For all branched molecules, the following two relations are found to hold always:

$$\sum_{n=1}^{r-1} \delta_{r \rightarrow n} = 2(r-1) \quad (23a)$$

$$\sum_{n=1}^{r-1} n \delta_{r \rightarrow n} = r(r-1) \quad (23b)$$

Table 1 Generation of the Forward and Reverse Backbone Indices

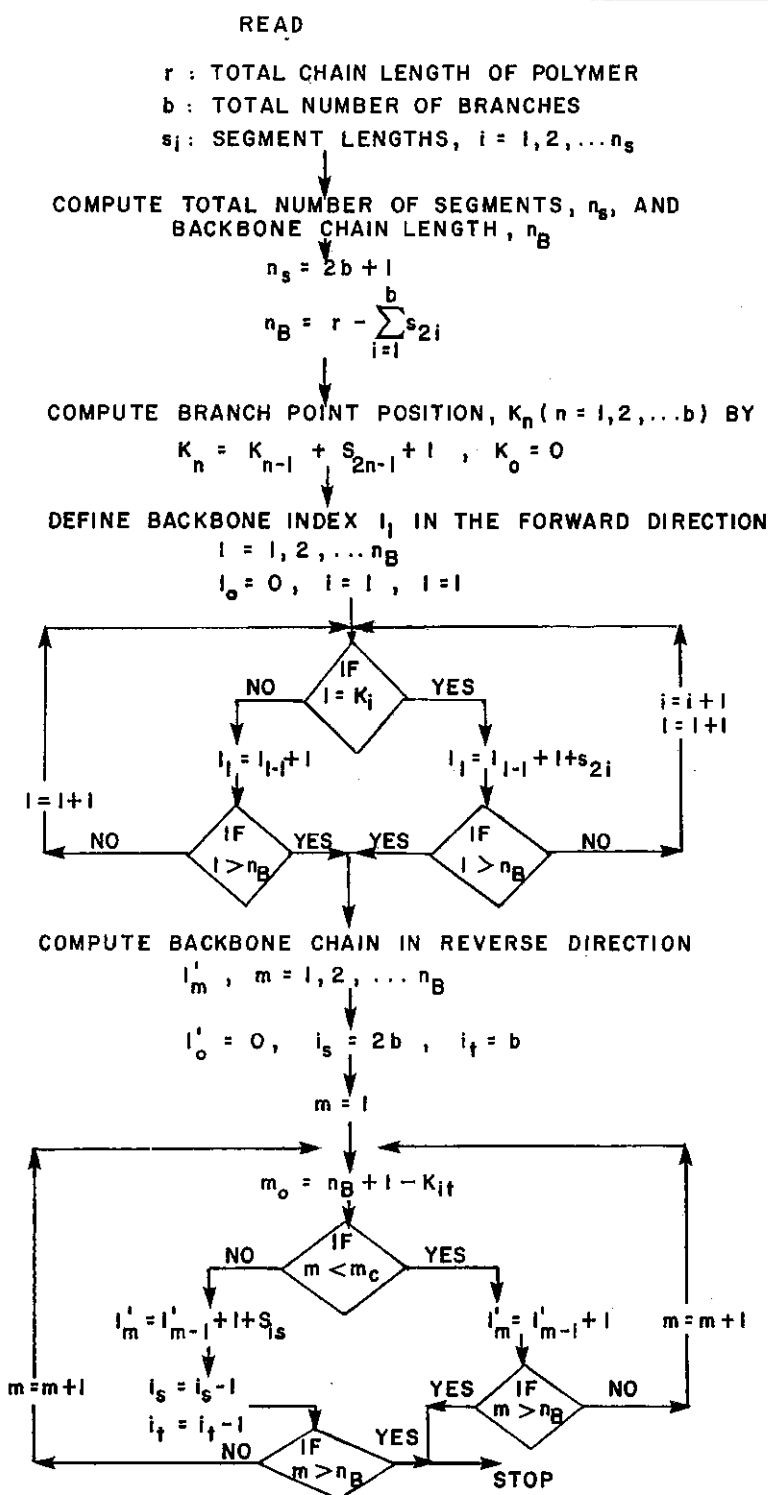
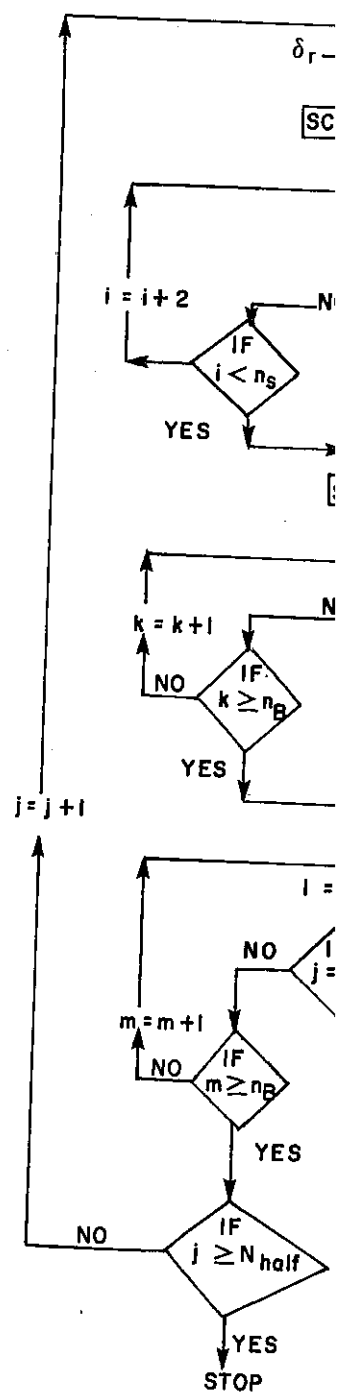


Table 2 Calculation of  $\delta_{r \rightarrow n}$

READ  $r, s_i, I_i$  &

$N_i$



\_\_\_\_\_ (Signature)

\_\_\_\_\_

1

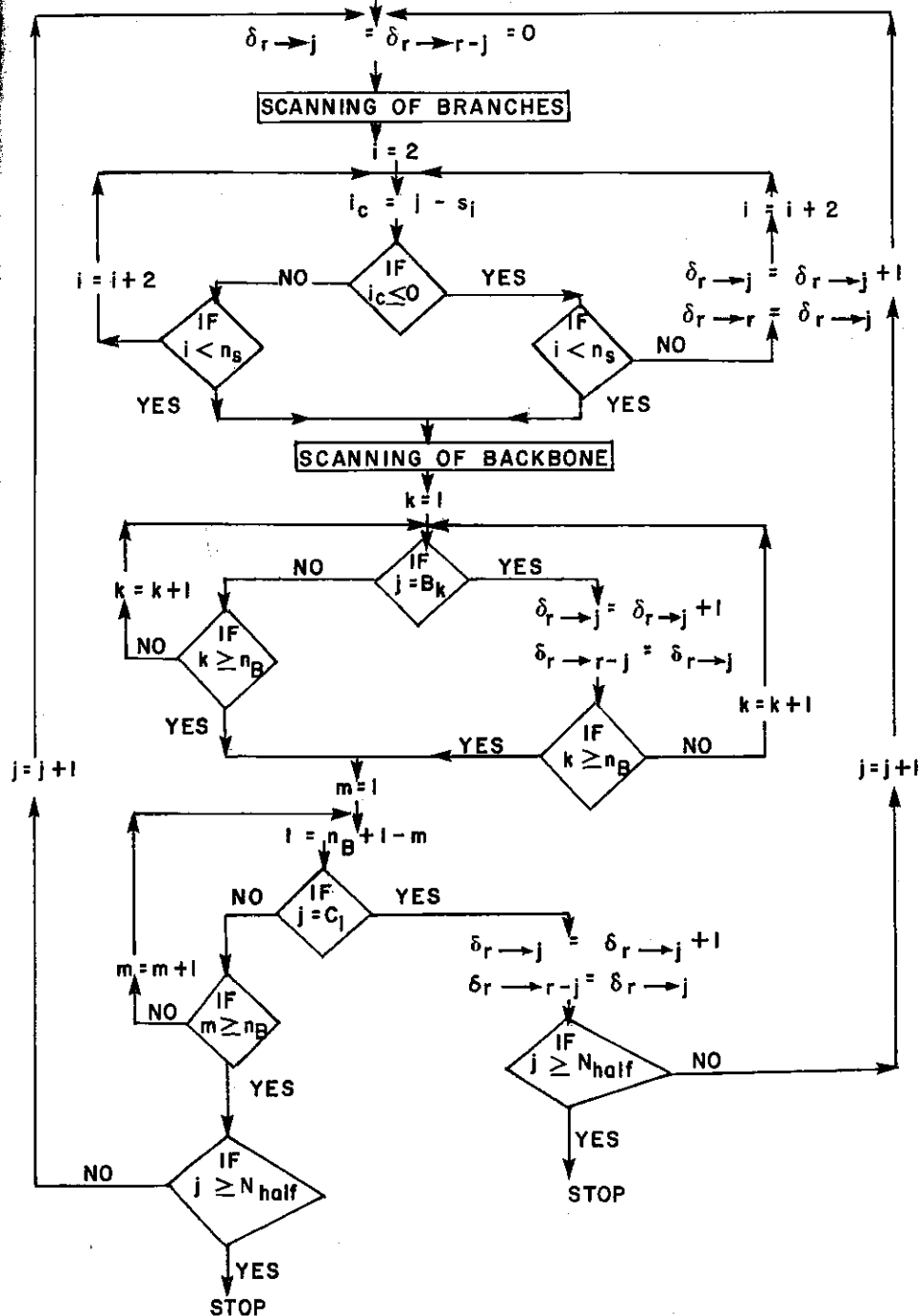


**Table 3** Value of  $\delta_{r \rightarrow n}$  for Different Branched Structures Seen in Figure 6

$n$	$\delta_{17 \rightarrow n}$ for Fig 6a	$\delta_{17 \rightarrow n}$ for Fig 6b	$\delta_{17 \rightarrow n}$ for Fig 6c	$\delta_{17 \rightarrow n}$ for Fig 6d	$\delta_{17 \rightarrow n}$ for Fig 6e	$\delta_{17 \rightarrow n}$ for Fig 6f
1	2	4	5	5	4	3
2	2	4	5	4	4	3
3	2	4	0	2	4	3
4	2	4	0	1	1	3
5	2	0	2	1	0	2
6	2	0	2	1	0	2
7	2	0	2	1	1	0
8	2	0	0	1	2	0
9	2	0	0	1	2	0
10	2	0	2	1	1	0
11	2	0	2	1	0	2
12	2	0	2	1	0	2
13	2	4	0	1	1	3
14	2	4	0	2	4	3
15	2	4	5	4	4	3
16	2	4	5	5	4	3

However, the summation  $\sum_{n=1}^{r-1} n^2 \delta_{r \rightarrow n}$  depends on the structure. If the chain structure is that given in Figure 6c, then

$$\sum_{n=1}^{r-1} n^2 \delta_{r \rightarrow n} = A_1 r^3 + A_2 r^2 + A_3 r + A_4 \quad (24)$$

where

$$A_1 = \frac{(20b^3 + 24b^2 + 14b + 2)}{3(2b + 1)^3} \quad (25a)$$

$$A_2 = -\frac{(8b^4 + 64b^3 + 88b^2 + 32b + 6)}{6(2b + 1)^3} \quad (25b)$$

$$A_3 = \frac{(16b^4 + 30b^3 + 26b^2 + 16b + 2)}{6(2b + 1)^3} \quad (25c)$$

$$A_4 = -\frac{(2b^4 + 9b^3 + b^2)}{6(2b + 1)^3} \quad (25d)$$

It is observed that the relations given in Eqs. 25 are independent of the functionality  $f$  of the starting monomer. If there are no intramolecular reactions, there would be  $nf - 2(n - 1)$  unreacted Y groups on  $P_n$  because for every bond formed, two Y groups are consumed. Two reacting molecular species  $P_n$  and  $P_m$  have  $f_1 = [nf - 2(n - 1)]$  and  $f_2 = [mf - 2(m - 1)]$  unreacted functional groups on them. When they undergo reaction, there are  $f_1 f_2 / 2$  distinct ways by which they can react. The factor of  $1/2$  is included because the reactive groups Y are identical. For any general species  $P_n$  produced according to Eq. 3

the mole balance relation be derived as

$$\frac{d[P_1]}{dt} = 2k_p(a + 1)$$

$$\frac{d[P_n]}{dt} = k_p \sum_{r=1}^{n-1} (ar -$$

$$-2k_p(an +$$

$$-k'_p[P_n][W]$$

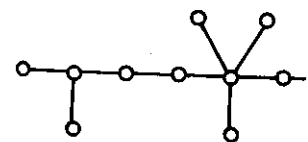
$$a = \frac{f - 2}{2}$$

Equations 26 involve the reacting polymer chains, the chain structure.

A functional group approach to polymer in the reaction involves collision of two oligomer chains. Whenever reactive branch is produced at that point, a hexafunctional monomer is involved in the polymerization through the analysis of bifunctional structure.

In the functional group approach to follow the polymerization of species A to G as shown in Figure 7, the number of unreacted reactive groups on a polymer chain is the same to the monomer. As species B has only one functional group, it is the same to the monomer. Species C forms the chain structure. It is possible to follow the polymerization to G very conveniently.

Various forward and reverse

**Figure 7** General structure of



in Figure 6

$i$	$\delta_{17 \rightarrow n}$ for Fig 6e	$\delta_{17 \rightarrow n}$ for Fig 6f
	4	3
	4	3
	4	3
	1	3
	0	2
	0	2
	1	0
	2	0
	2	0
	1	0
	0	2
	0	2
	1	3
	4	3
	4	3
	4	3

ture. If the chain structure is

(24)

(25a)

(25b)

(25c)

(25d)

ent of the functionality  $f$  of  
there would be  $nf - 2(n -$   
vo Y groups are consumed.  
 $2(n - 1)]$  and  $f_2 = [mf -$   
ndergo reaction, there are  
/2 is included because the  
duced according to Eq. 3

the mole balance relation for the step growth polymerization in the batch reactor can now be derived as

$$\frac{d[P_1]}{dt} = 2k_p(a + 1)[P_1] \left\{ \sum_{m=1}^{\infty} (am + 1)[P_m] \right\} + k'_p[W] \sum_{r=2}^{\infty} \delta_{r \rightarrow 1}[P_r] \quad (26a)$$

$$\begin{aligned} \frac{d[P_n]}{dt} = & k_p \sum_{r=1}^{n-1} (ar + 1)\{a(n - r) + 1\}[P_r][P_{n-r}] \\ & - 2k_p(an + 1)[P_n] \sum_{m=1}^{\infty} (am + 1)[P_m] \\ & - k'_p[P_n][W](n - 1) + k'_p[W] \sum_{r=n+1}^{\infty} \delta_{r \rightarrow n}[P_r] \quad \text{for } n \leq 2 \end{aligned} \quad (26b)$$

$$a = \frac{f - 2}{2} \quad (26c)$$

Equations 26 involve the term  $\delta_{r \rightarrow n}$ , which is dependent on the number of branches in the reacting polymer chains. This implies that Eqs. 26 cannot be solved without knowledge of the chain structure.

A functional group approach is now discussed in order to find the average branching of polymer in the reaction mass. Consider a hexafunctional monomer ( $f = 6$ ). At every collision of two oligomers, two reactive groups are eliminated to form a bond between them. Whenever reactive groups in the middle of the chain undergo chemical reaction, a branch is produced at that point. A general chain structure produced by the polymerization of a hexafunctional monomer is shown in Figure 7. It is possible to follow the course of polymerization through the functional group approach, which is a generalization of Flory's analysis of bifunctional step growth polymerization.

In the functional group approach, one defines  $(f + 1)$  functional group species in order to follow the polymerization of  $RY_f$  monomers. As an example, one would require seven species A to G as shown in Figure 8. These differ from each other in terms of the number of unreacted reactive groups Y on them. For example, A has all reactive groups unreacted and is the same to the monomer while B has one reacted reactive group, C has two, and so on. As species B has only one of its reactive group reacted, it can be situated only at chain ends. Species C forms the linear part of the chain, while the other species lead to branching. It is possible to represent the chain structure of Figure 7 in terms of species B to G very conveniently.

Various forward and reverse reactions leading to polymer formation involving these

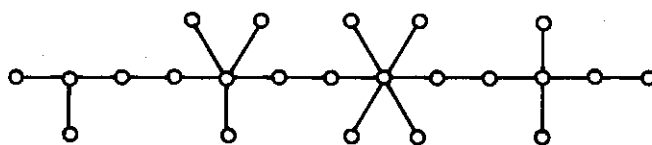


Figure 7 General structure of polymer chain in the polymerization of hexafunctional monomer.

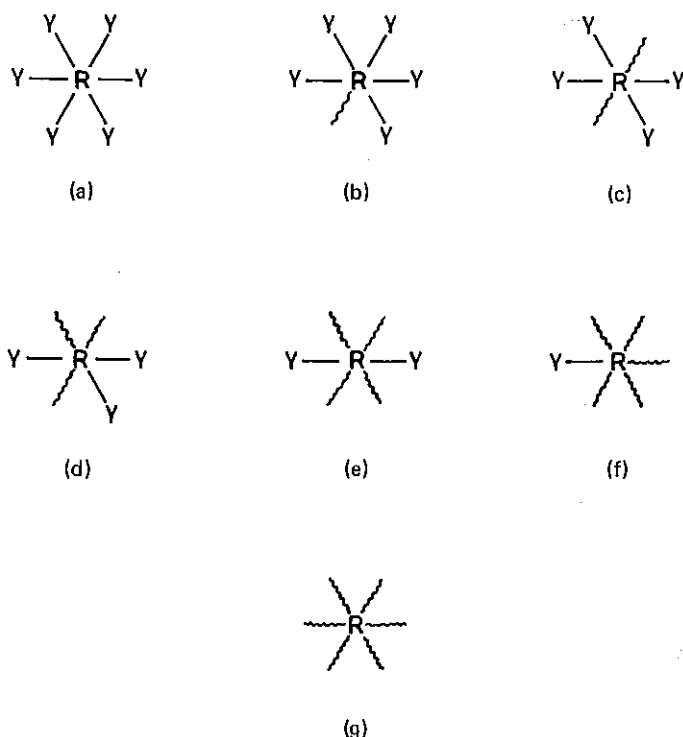


Figure 8 Structures of functional group species.

functional group species can be easily written and are summarized in Table 4. In writing these, it has been assumed that all species are available for chemical reaction with equal likelihood. It is assumed that species A reacts with C. There is a chemical reaction of reactive groups Y on species A with those of species C; when this occurs, species A would become B because one of its reactive group is reacted while C becomes D for the same reason. In view of this, the forward step of the reaction between species A and C can be represented as



on the right-hand side B appears in parentheses to indicate that B is not free but is in the combined state as B-D.

To determine the reactivity  $k_3$  (see Table 4), it is observed that reaction between any two species occurs only when they collide. If the collision frequency between species A and C is represented  $Z_{AC}$  and  $Q_{AC}$  as the probability of reaction between A and C, then rate  $\mathcal{R}_{AC}$  is given as

$$\mathcal{R}_{AC} = \alpha Z_{AC} Q_{AC} \quad (28)$$

where  $\alpha$  is the constant of proportionality. For equal reactivity of reactive groups Y,  $Z_{AC}$  would be given by  $[(6 \times 4)/2Z]$  where Z is the probability of reaction between Y's of the two species A and C. The factor  $(6 \times 4)/2$  arises because species A has six and species C

Table 4 Various Reactions of

## Forward Reactions

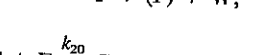
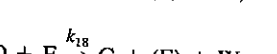
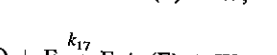
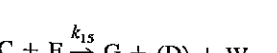
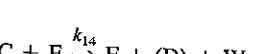
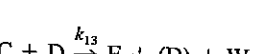
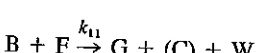
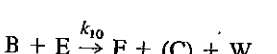
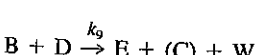
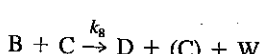
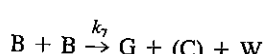
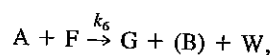
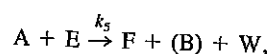
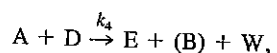
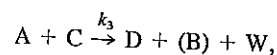
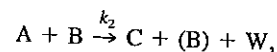
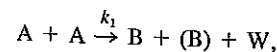
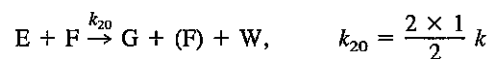
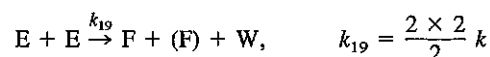
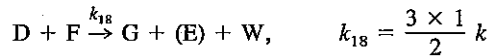
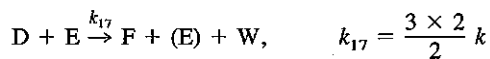
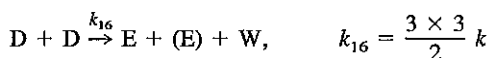
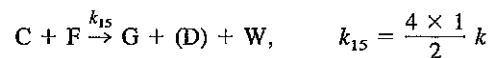
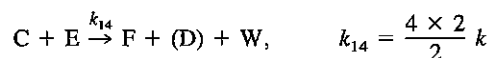
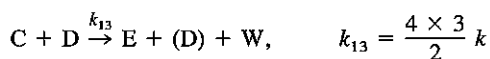
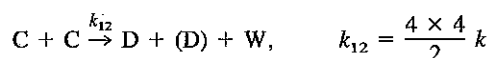
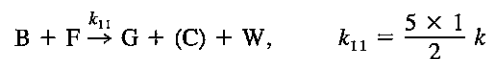
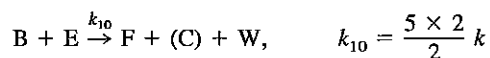
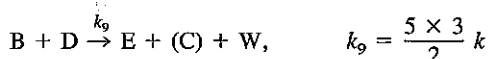
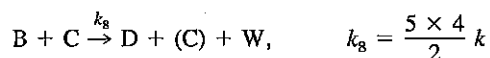
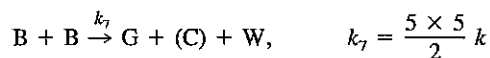
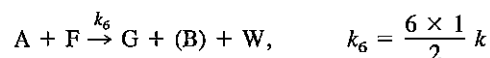
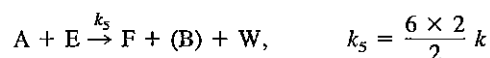
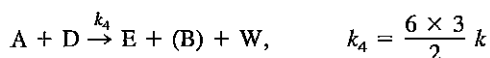
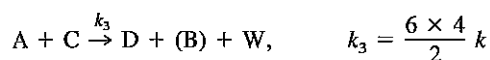
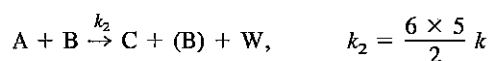
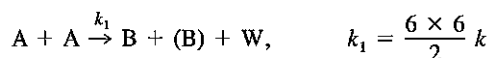


Table 4 Various Reactions of Species A to G

## Forward Reactions



arized in Table 4. In writing  
chemical reaction with equal  
re is a chemical reaction of  
this occurs, species A would  
C becomes D for the same  
een species A and C can be

(27)

at B is not free but is in the

d that reaction between any  
equency between species A  
ion between A and C, then

(28)

y of reactive groups Y,  $Z_{AC}$   
reaction between Y's of the  
ies A has six and species C

Table 4 (Continued)

$F + F \xrightarrow{k_{21}} G + (G) + W,$	$k_{21} = \frac{1 \times 1}{2} k$
<i>Reverse Reactions</i>	
$B + (B) + W \xrightarrow{k'_1} A + A,$	$k'_1 = \frac{[B]}{XX} k'$
$B + (C) + W \xrightarrow{k'_2} A + B,$	$k'_2 = \frac{[C]}{XX} k'$
$B + (D) + W \xrightarrow{k'_3} A + C,$	$k'_3 = \frac{[D]}{XX} k'$
$B + (E) + W \xrightarrow{k'_4} A + D,$	$k'_4 = \frac{[E]}{XX} k'$
$B + (F) + W \xrightarrow{k'_5} A + E,$	$k'_5 = \frac{[F]}{XX} k'$
$B + (G) + W \xrightarrow{k'_6} A + F,$	$k'_6 = \frac{[G]}{XX} k'$
$C + (C) + W \xrightarrow{k'_7} B + B,$	$k'_7 = 2 \frac{[C]}{XX} k'$
$C + (D) + W \xrightarrow{k'_8} B + C,$	$k'_8 = 2 \frac{[D]}{XX} k'$
$C + (E) + W \xrightarrow{k'_9} B + D,$	$k'_9 = 2 \frac{[E]}{XX} k'$
$C + (F) + W \xrightarrow{k'_{10}} B + E,$	$k'_{10} = 2 \frac{[F]}{XX} k'$
$C + (G) + W \xrightarrow{k'_{11}} B + F,$	$k'_{11} = 2 \frac{[G]}{XX} k'$
$D + (D) + W \xrightarrow{k'_{12}} C + C,$	$k'_{12} = 3 \frac{[D]}{XX} k'$
$D + (E) + W \xrightarrow{k'_{13}} C + D,$	$k'_{13} = 3 \frac{[E]}{XX} k'$
$D + (F) + W \xrightarrow{k'_{14}} C + E,$	$k'_{14} = 3 \frac{[F]}{XX} k'$
$D + (G) + W \xrightarrow{k'_{15}} C + F,$	$k'_{15} = 3 \frac{[G]}{XX} k'$
$E + (E) + W \xrightarrow{k'_{16}} D + D,$	$k'_{16} = 4 \frac{[E]}{XX} k'$
$E + (F) + W \xrightarrow{k'_{17}} D + E,$	$k'_{17} = 4 \frac{[F]}{XX} k'$
$E + (G) + W \xrightarrow{k'_{18}} D + F,$	$k'_{18} = 4 \frac{[G]}{XX} k'$

Table 4 (Continued)

$F + (F) + W \xrightarrow{k'_{19}} E + E,$
$F + (G) + W \xrightarrow{k'_{20}} E + F,$
$G + (G) + W \xrightarrow{k'_{21}} F + F,$

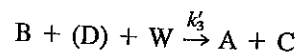
Note:  $XX = [B] + [C] + [D] + [E] + [F] + [G]$

has four reactive groups and  $(6 \times 4)/2$ . Since the collision is between two species, it implies that the reaction rate is

$$k_3 = \frac{6 \times 4}{2} k$$

where  $k$  is the reactivity of the functional group. The forward steps have been derived from the reverse reaction in mind.

The reverse reaction in mind is the breaking of bonds in functional group species. The complexity arises because we must have a bond broken. One considers bond B-D reaction, but simultaneously D would be broken. Even though in reality it is only one reaction of any given functional group, it must be available. The reverse reaction rate is given by



The rate constant for this step is given in terms of the reverse reaction rate constant. To derive the rate constant for species B has only one reactive group, the reverse rate  $\mathcal{R}'_{B(D)}$  is given by

$$\mathcal{R}'_{B(D)} = k'[B][W]P_{B(D)}$$

where  $P_{B(D)}$  is the probability of finding species B can be found adjacent to species D.

$$P_{B(D)} = \frac{[D]}{[B] + [C] + [D] + [E] + [F] + [G]}$$

With this background and the mole balance relations for these species, the given by

Table 4 (Continued)

$F + (F) + W \xrightarrow{k'_{19}} E + E,$	$k'_{19} = 5 \frac{[F]}{XX} k'$
$F + (G) + W \xrightarrow{k'_{20}} E + F,$	$k'_{20} = 5 \frac{[G]}{XX} k'$
$G + (G) + W \xrightarrow{k'_{21}} F + F,$	$k'_{21} = 6 \frac{[G]}{XX} k'$

Note:  $XX = [B] + [C] + [D] + [E] + [F] + [G]$ .

has four reactive groups and the distinct combinations of two Y groups between them is  $(6 \times 4)/2$ . Since the collision frequency between species A and C is proportional to  $[A][C]$ , it implies that the reactivity  $k_3$  for this step is given by

$$k_3 = \frac{6 \times 4}{2} k \quad (29)$$

where  $k$  is the reactivity of Y groups. Using similar logic the rate constants of all the forward steps have been derived and included in Table 4.

The reverse reaction in multifunctional polymerization involves the reaction of the bonds in functional group species with the condensation product, W. However, complexity arises because we must have knowledge of the neighborhood species. For example, one considers bond B–D reacting with W. In the reverse reaction step, B would become A, but simultaneously D would become C. Thus it appears to be a trimolecular reaction even though in reality it is only bimolecular in nature. If attention is focused on the reverse reaction of any given functional group species, knowledge of the connecting species must be available. The reverse reaction step can be written as



The rate constant for this step in Table 4 has been shown to be  $k'_3$  and it is desired to write this in terms of the reverse rate constant  $k'$  between given reaction Y group and the condensation product W. To do so, the reaction is taken as that between B and W. Since species B has only one reacted bond in it, its reactivity would therefore be  $k'$  and the reverse rate  $\mathcal{R}'_{B(D)}$  is given by

$$\mathcal{R}'_{B(D)} = k'[B][W]P_{B(D)} \quad (31)$$

where  $P_{B(D)}$  is the probability of finding D adjacent to species B. If it is assumed that any species can be found adjacent to B, this probability term can be approximated as

$$P_{B(D)} = \frac{[D]}{[B] + [C] + [D] + [E] + [F] + [G]} \quad (32)$$

With this background and the kinetic scheme given in Table 4, it is possible to write the mole balance relations for these functional group species in batch reactors. These are given by

$$\frac{d[A]}{dt} = -3k[A][M] + k'[B][M] \quad (33a)$$

$$\frac{d[B]}{dt} = 3k[A][M] - \frac{5}{2}k[B][M] + 2k'[C][W] - k'[B][W] \quad (33b)$$

$$\frac{d[C]}{dt} = \frac{5}{2}k[B][M] - 2k[C][M] + 3k'[D][W] - 2k'[C][W] \quad (33c)$$

$$\frac{d[D]}{dt} = 2k[C][M] - \frac{3}{2}k[D][M] + 4k'[E][W] - 3k'[D][W] \quad (33d)$$

$$\frac{d[E]}{dt} = \frac{3}{2}k[D][M] - k[E][M] + 5k'[F][W] - 4k'[E][W] \quad (33e)$$

$$\frac{d[F]}{dt} = k[E][M] - \frac{k}{2}[F][M] + 6k'[G][W] - 5k'[F][W] \quad (33f)$$

$$\frac{d[G]}{dt} = \frac{k}{2}[F][M] - 6k'[G][W] \quad (33g)$$

$$\begin{aligned} \frac{d[W]}{dt} = k[M] \left\{ \frac{3}{2}[A] + \frac{5}{4}[B] + [C] + \frac{3}{4}[D] + \frac{[E]}{2} + \frac{[F]}{4} \right\} \\ - k'[W] \left\{ \frac{[B]}{2} + [C] + \frac{3}{2}[D] + 2[E] + \frac{5}{2}[F] + 3[G] \right\} \end{aligned} \quad (33h)$$

where

$$[M] = 6[A] + 5[B] + 4[C] + 3[D] + 2[E] + [F] \quad (33i)$$

Once the concentrations of the functional group species are known the average branches present in the reaction mass can be determined in the following way. Species D, E, F, and G have 1, 2, 3, and 4 branches, respectively. The average number of branches present in the reaction mass can be given by

$$\bar{b} = \frac{[D] + 2[F] + 3[F] + 4[G]}{\sum_{n=1}^{\infty} [P_n]} \quad (34)$$

Computations have shown that in multifunctional polymerization, the concentration of the higher functional group species E to G are present in negligible concentrations compared to B to D all the way up to the gel point. Thus an average structure (as shown in Fig. 6c) can be assumed without introducing any error in computations.

In multifunctional polymerization one is mainly interested in the moments of the distribution instead of the entire MWD. Equation 21 can be added according to Eq. 1 for all  $n$  to obtain the moment generation results. With the help of Eq. 47, the following relations are derived:

$$\frac{d\lambda_0}{dt} = k(a\lambda_1 + \lambda_0)^2 + k'[W](\lambda_1 - \lambda_0) \quad (35a)$$

$$\frac{d\lambda_1}{dt} = 0 \quad (35b)$$

$$\begin{aligned} \frac{d\lambda_2}{dt} = 2k(a\lambda_2 + \lambda_1)^2 + k'[W]\{(A_2 + 1)\lambda_2 + A_3\lambda_1 + A_4\lambda_0\} \\ + k'[W](A_1 - 1)\lambda_3 \end{aligned} \quad (35c)$$

Equation 35c is dependent on some moment closure relation.

Using the computer algorithm for various  $n$  ( $n = 1, 2, \dots$ ), structures. The table shows balance relations involve 8 affected by the branching. strated for the batch polymer functional group species (Fig small for the conversion of r average branching so generat In Figure 9, concentrations o of polymerization  $t'$  as a para

Examination of Figure 9 becomes broader. This is expected to increase. In Figure for different equilibrium cons ible polymerization and for reactive groups is achieved.

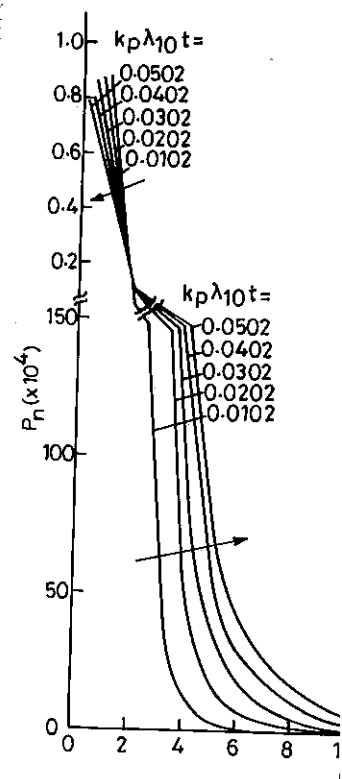


Figure 9 Dimensionless concentration

Equation 35c is dependent on the higher moment  $\lambda_3$  and can be solved only after assuming some moment closure relation as is done for linear polymerization.

Using the computer algorithm for  $\delta_{r \rightarrow n}$ ,  $r$  was fixed at 17. This was calculated for various  $n$  ( $n = 1, 2, \dots, 16$ ), and results are presented in Table 3 for different chain structures. The table shows an extreme sensitivity to the chain structure. Since the mole balance relations involve  $\delta_{r \rightarrow n}$ , the MWD of the polymer is expected to be greatly affected by the branching. The computation technique outlined here has been demonstrated for the batch polymerization of hexafunctional monomers. For this we need seven functional group species (Fig. 8); their numerical solution shows that the total branching is small for the conversion of reactive groups below the gel point. With the information on average branching so generated, it is now possible to determine the MWD of the polymer. In Figure 9, concentrations of  $P_n$  species versus chain length  $n$  were plotted with the time of polymerization  $t'$  as a parameter.

Examination of Figure 9 reveals that as the reaction time  $t'$  increases, the MWD becomes broader. This is expected with increasing time, higher oligomers are formed in larger concentrations and both the average chain length and the polydispersity index  $\rho$  are expected to increase. In Figure 10, the MWD of a given time of polymerization is plotted for different equilibrium constants,  $K$ . As  $K$  is increased, the reaction is closer to irreversible polymerization and for a given time of polymerization, a higher conversion of reactive groups is achieved. This would in turn imply that the MWD would become

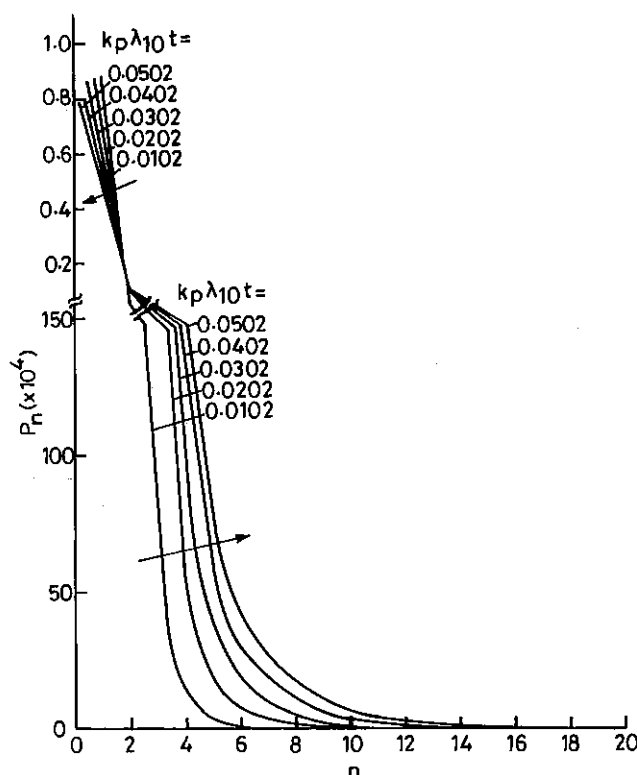


Figure 9 Dimensionless concentration of  $P_n$  species versus  $n$  ( $t$  varies from 0.0102 to 0.0502).

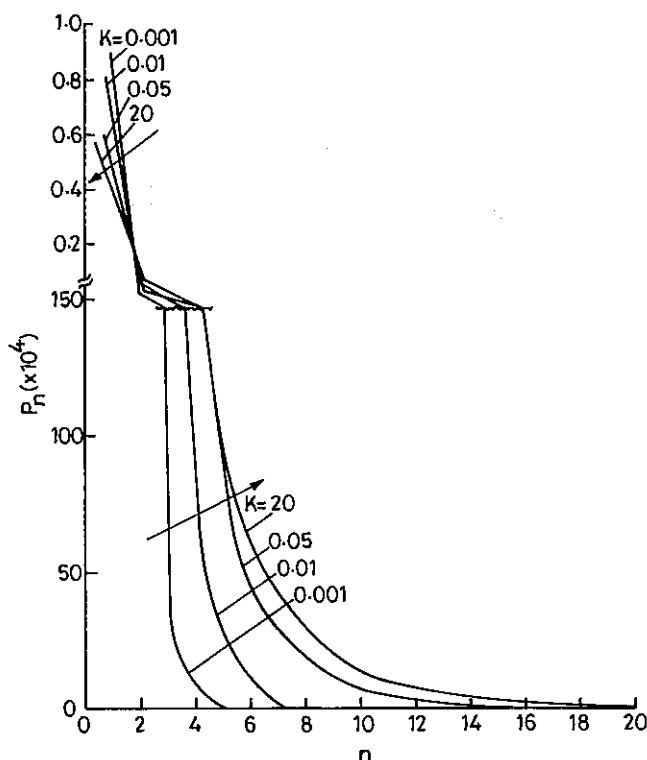


Figure 10 Dimensionless concentration of  $P_n$  species versus  $n$  ( $K$  varies from 0.0 to 20).

broader for increasing  $K$ , which is indeed seen in this figure. From the MWD results, it is possible to calculate the moments  $\lambda_0$  and  $\lambda_2$  (defined in Eq. 1). Theoretically (also found computationally), the first moment  $\lambda_1$  is time invariant; thus the number and weight average chain lengths  $\mu_n$  and  $\mu_w$  and the polydispersity index  $p$  can be determined. It is found that the overall polymerization is limited by equilibrium conversion, which increases with increasing  $K$ . It is further observed from Eqs. 18 that for a given  $r$ ,  $\delta_{r \rightarrow n}$  is  $(b + 2)$  for small  $n$ , which implies that as the degree of branching  $b$  increases, smaller chains (and therefore large chains due to symmetry) are formed preferentially. This would give rise to a higher polydispersity index compared to those formed from irreversible polymerization at the same conversion of reactive groups. An example, for  $K = 0.1$ , at conversion of 13.87% the polydispersity index is 2.10; for the same conversion for irreversible polymerization it is 1.89.

In deriving an expression for  $\sum_{n=1}^{\infty} n^2 \delta_{r \rightarrow n}$  in Eqs. 25, a specific chain structure as in Figure 6c was assumed. Computations for noninteger segment length  $x$  and noninteger number of branches were tested against wide variations of parameters. Noninteger  $x$  in actuality amounts to stating that all segment lengths are not of equal length. If the chain length  $r$  and the number of branches  $b$  (whole numbers here) are given,  $x$  can be calculated as

$$x = \frac{r - b}{2b + 1} \quad (36)$$

If  $x$  calculated this way is a noninteger (in this case 6) and  $r^*$  is calculated as

$$r^* = (2b + 1)x^*$$

The remainder  $(r - r^*)$  represents the number of chain structure,  $\delta_{r \rightarrow n}$  can be calculated exactly  $\sum_{n=1}^{\infty} n^2 \delta_{r \rightarrow n}$  with that. On similar testing for fractions and those from Eq. 24 is negligible.

The generation relation for  $\lambda_3$ . To solve it, a moment closure is assumed irreversible, the MWD is exactly and is given by

$$\frac{[P_n]}{[P]_0} = \frac{\{n(f - 1)\}!}{n! \{(f - 2)n + 2\}!}$$

where  $p$  is the conversion of the polymerization of hexafunctional groups.

$$\lambda_3 = \frac{(1 + p - 7p^2 + 5p^3)}{(1 - p)^3}$$

which can serve as a moment closure. The MWD relations given in Eqs. 24 and 25 are used to obtain results using the empirical relation

$$\ln \lambda_3 = a_1 + a_2 \ln \lambda_0 + a_3 \ln \lambda_2$$

where  $a_1$  and  $a_3$  are the curve-fitting parameters.

$$\lambda_3 = \frac{1.036 \lambda_2^{1.45}}{\lambda_0^{2.67}}$$

With the moment closure approach,  $\lambda_2$  and its values compared with experimental data for given  $K$ , Eq. 41 serves as a good approximation for gel point conversions. As the gel point conversion is represented, as can be seen in Figure 10.

With the developments outlined above, the equilibrium in multifunctional step polymerization, their moments would be calculated, as shown in Eq. 35a, for the zeroth moment,

$$K = \frac{k}{k'} = \frac{[W](\lambda_1 - \lambda_0)}{(a\lambda_1 + \lambda_0)^2}$$

Since the condensation product of the polymerization for  $\lambda_0^0$  moles of reactive groups is

$$[W] = \lambda_0^0 - \sum_{n=1}^{\infty} [P_n] = \lambda_0^0 - \sum_{n=1}^{\infty} [P_n]$$



If  $x$  calculated this way is a noninteger (say 6.7), the lower integer value  $x^*$  of  $x$  is chosen (in this case 6) and  $r^*$  is calculated as

$$r^* = (2b + 1)x^* \quad (37)$$

The remainder  $(r - r^*)$  repeat units are distributed on various chain segments. For this chain structure,  $\delta_{r \rightarrow n}$  can be computed using the algorithm of Table 2. On comparing the exact  $\sum_{r=1}^n n^2 \delta_{r \rightarrow n}$  with that determined from Eq. 24, results are found to be within 1%. On similar testing for fractional branching  $b$ , the discrepancy between the exact results and those from Eq. 24 is negligible.

The generation relation for the second moment  $\lambda_2$  in Eqs. 26 involves third moment  $\lambda_3$ . To solve it, a moment closure relation for  $\lambda_3$  is needed. If the polymerization is assumed irreversible, the MWD in multifunctional self-polymerization can be solved exactly and is given by

$$\frac{[P_n]}{[P]_0} = \frac{\{n(f-1)\}!}{n! \{(f-2)n+2\}!} f p^{n-1} (1-p)^{n(f-2)+2} \quad (38)$$

where  $p$  is the conversion of reactive groups. From this, the third moment for the polymerization of hexafunctional monomers can be derived as

$$\lambda_3 = \frac{(1+p-7p^2+5p^3) + (1-5p)^2 2p\lambda_2}{(1-5p)^3} \quad (39)$$

which can serve as a moment closure approximation. From the numerical solution of the MWD relations given in Eqs. 26, one can also find  $\lambda_0$ ,  $\lambda_1$ ,  $\lambda_2$ , and  $\lambda_3$  and curve-fit these results using the empirical relation

$$\ln \lambda_3 = a_1 + a_2 \ln \lambda_0 + a_3 \ln \lambda_2 \quad (40)$$

where  $a_1$  and  $a_3$  are the curve-fit constants to be determined. On doing this we find that

$$\lambda_3 = \frac{1.036 \lambda_2^{1.45}}{\lambda_0^{2.67}} \quad (41)$$

With the moment closure approximations in Eqs. 39 and 41, Eq. 35c has been solved for  $\lambda_2$  and its values compared with those found from the MWD results. It is found that for a given  $K$ , Eq. 41 serves as a good approximation provided the conversion is well below the gel point conversions. As the gel point conversion is approached, Eq. 39 serves as a good representation, as can be seen in Table 5.

With the developments outlined in this work, it is now possible to analyze the equilibrium in multifunctional step growth polymerization. Since at equilibrium the MWD is stationary, their moments would also be time invariant, or  $d\lambda_i/dt = 0$  ( $i = 1, 2, \dots$ ). From Eq. 35a, for the zeroth moment, we obtain

$$K = \frac{k}{k'} = \frac{[W](\lambda_1 - \lambda_0)}{(a\lambda_1 + \lambda_0)^2} \quad (42)$$

Since the condensation product does not leave the reaction mass, the stoichiometry of the polymerization for  $\lambda_0^0$  moles of monomer initially present is given by

$$[W] = \lambda_0^0 - \sum_{n=1}^{\infty} [P_n] = \lambda_0^0 - \lambda_0 \quad (43)$$

$K$  varies from 0.0 to 20).

From the MWD results, it is 1). Theoretically (also found thus the number and weight ex  $p$  can be determined. It is brium conversion, which in- 18 that for a given  $r$ ,  $\delta_{r \rightarrow n}$  is anching  $b$  increases, smaller ed preferentially. This would ose formed from irreversible n an example, for  $K = 0.1$ , at for the same conversion for

specific chain structure as in nent length  $x$  and noninteger parameters. Noninteger  $x$  in : of equal length. If the chain e) are given,  $x$  can be calcu-

**Table 5** Comparison of  $\lambda_2$  Values Obtained by Using Three Different  $\lambda_3$  Expressions Given by Eqs. 39–41

Time	Conversion (%)	$\lambda_2$ Values			
		By MWD	Using Flory-Schulz relation for $\lambda_3$	Using Stockmayer relation for $\lambda_3$	Using Eq. 41 for $\lambda_3$
For $K = 0.1$					
0.0012	0.3586	1.02191	1.02191	1.02192	1.02191
0.0102	2.9600	1.20845	1.20860	1.20852	1.20841
0.0202	5.6483	1.47215	1.47379	1.47255	1.47217
0.0302	8.1048	1.81644	1.82477	1.81760	1.81718
0.0402	10.3214	2.27229	2.30387	2.27445	2.27703
0.0502	12.2970	2.87917	2.98653	2.88106	2.90465
0.0552	13.1950	3.25250	3.44561	3.24940	3.30720
0.0592	13.8720	3.58946	3.89488	3.57228	3.68610
For $K = 0.02$					
0.0012	0.358623	1.02191	1.02191	1.02192	1.02191
0.0102	2.92437	1.20550	1.20619	1.20583	1.20530
0.0202	5.40353	1.44374	1.45101	1.44552	1.44374
0.0302	7.40084	1.70129	1.73204	1.70549	1.70354
0.0402	8.92173	1.95266	2.03790	1.95538	1.96110
0.0502	10.03150	2.17232	2.35367	2.15412	2.19195
0.0602	10.81690	2.34623	2.66384	2.25357	2.37890
0.0702	11.3609	2.47397	2.95522	2.19925	2.51586
0.0802	11.7348	2.56466	3.21877	1.92928	2.60580
0.0902	11.9599	2.61093	3.44994	1.38786	2.65666
0.1052	12.1603	2.65038	3.73493	0.065054	2.67934
For $K = 0.01$					
0.0012	0.3585	1.02190	1.02191	1.02192	1.02190
0.0102	2.88118	1.20194	1.20329	1.20258	1.20155
0.0202	5.13143	1.41337	1.42601	1.41643	1.41322
0.0302	6.70479	1.60084	1.64567	1.60678	1.60344
0.0402	7.70824	1.74085	1.84022	1.74353	1.7483
0.0502	8.31215	1.83239	1.99886	1.86508	1.84459
0.0602	8.66409	1.88767	2.12117	1.89569	1.90176
0.0702	8.85234	1.91398	2.21235	1.94470	1.93246
0.0802	8.95715	1.92876	2.27917	1.90999	1.94689
0.1024	9.05435	1.94282	2.36902	1.86951	1.95117
0.1194	9.07846	1.94649	2.40623	1.64685	1.94443
For $K = 0.0025$					
0.0012	0.35802	1.02187	1.02188	1.02192	1.02183
0.0102	2.65117	1.18330	1.18779	1.18540	1.18185
0.0202	4.00993	1.29997	1.32615	1.30607	1.29796
0.0302	4.51773	1.34784	1.40186	1.35533	1.34683
0.0402	4.68372	1.36373	1.43904	1.36922	1.36377
0.0502	4.73626	1.36872	1.45737	1.36957	1.36941
0.0602	4.75310	1.37031	1.46673	1.36426	1.37150
0.0702	4.7580	1.37084	1.47167	1.35543	1.37223
0.0762	4.76011	1.37098	1.47346	1.34855	1.37243

For  $\lambda_0^0 = 1$ , the equilibrium

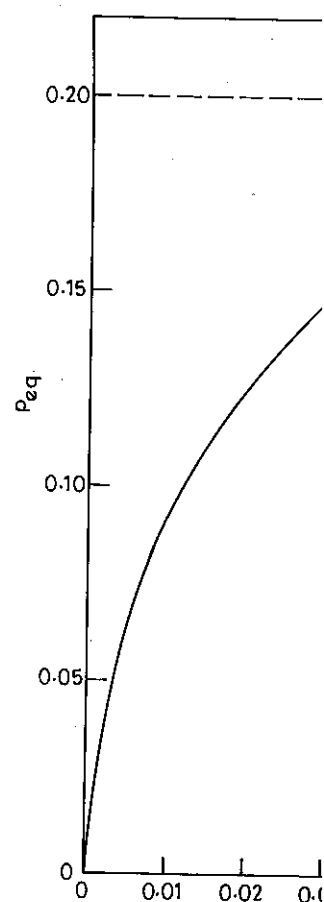
$$p_{eq} = \frac{\sqrt{K}}{1 + \sqrt{K}}$$

The second moment  $\lambda_2$  at eq

$$2(a\lambda_2 + \lambda_1)^2 + \frac{\lambda_0^0 - \lambda_1^0}{K} + \frac{(\lambda_0^0 - \lambda_1^0)}{K}$$

In Figure 11, equilibrium conversion reveals that it is independent of  $K$ . As  $K$  is increased,  $p_{eq}$  is increased, gelation would occur for  $K > 1$ .

In Table 6, equilibrium conversion and two-moment closure relation

**Figure 11** Equilibrium conversion

ifferent  $\lambda_3$  Expressions Given by

Using Stockmayer relation for $\lambda_3$	Using Eq. 41 for $\lambda_3$
1.02192	1.02191
1.20852	1.20841
1.47255	1.47217
1.81760	1.81718
2.27445	2.27703
2.88106	2.90465
3.24940	3.30720
3.57228	3.68610
1.02192	1.02191
1.20583	1.20530
1.44552	1.44374
1.70549	1.70354
1.95538	1.96110
2.15412	2.19195
2.25357	2.37890
2.19925	2.51586
1.92928	2.60580
1.38786	2.65666
0.065054	2.67934
1.02192	1.02190
1.20258	1.20155
1.41643	1.41322
1.60678	1.60344
1.74353	1.7483
1.86508	1.84459
1.89569	1.90176
1.94470	1.93246
1.90999	1.94689
1.86951	1.95117
1.64685	1.94443
1.02192	1.02183
1.18540	1.18185
1.30607	1.29796
1.35533	1.34683
1.36922	1.36377
1.36957	1.36941
1.36426	1.37150
1.35543	1.37223
1.34855	1.37243

For  $\lambda_0^0 = 1$ , the equilibrium conversion  $p_{eq}$  can be obtained as

$$p_{eq} = \frac{\sqrt{K}}{1 + \sqrt{K}} \quad (44)$$

The second moment  $\lambda_2$  at equilibrium can similarly be obtained by setting  $d\lambda_2/dt = 0$ , or

$$2(a\lambda_2 + \lambda_1)^2 + \frac{\lambda_0^0 - \lambda_0}{K} \{(A_2 + 1)\lambda_2 + A_3\lambda_1 + A_4\lambda_0\} + \frac{(\lambda_0^0 - \lambda_0)}{K} (A_1 - 1)\lambda_3 = 0 \quad (45)$$

In Figure 11, equilibrium conversion  $p_{eq}$  has been plotted as a function of  $K$ . Equation 44 reveals that it is independent of branching and is a monotonic function of  $K$ . As  $K$  is increased  $p_{eq}$  is increased, and for  $K = 0.0625$ ,  $p_{eq} = 0.20$ , which would mean that gelation would occur for hexafunctional monomers for any  $k$  greater than this value.

In Table 6, equilibrium weight average chain length  $\mu_{w,eq}$  has been computed for the two-moment closure relation in Eqs. 34 and 41. This table reveals that results are ex-

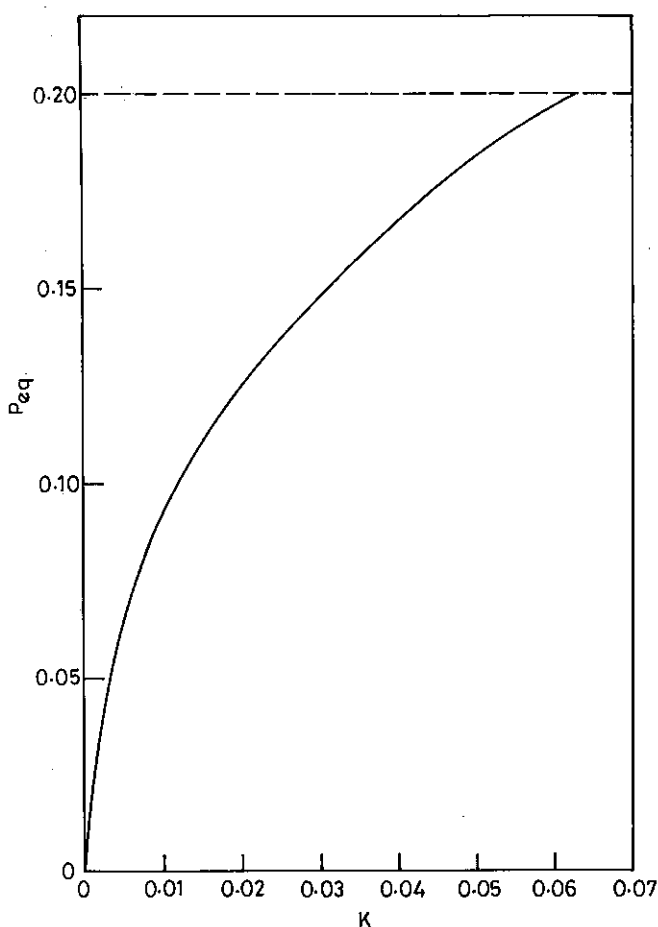


Figure 11 Equilibrium conversion,  $p_{eq}$ , versus  $K$ .

**Table 6** Comparison of  $\mu_{w,eq}$  Using Three Different Correlations for  $\lambda_3$  Given by Eqs. 39–41

K	$\mu_{w,eq}$ using Eq. 39	$\mu_{w,eq}$ using Eq. 40	$\mu_{w,eq}$ using Eq. 41
<i>b</i> = 0.02			
0.010	2.586	−4.293	−0.661
0.012	2.933	−10.293	1.579
0.020	4.910	111.668	3.168
0.030	11.585	111.879	4.626
0.040	44.029	112.202	6.609
0.050	213.104	113.728	9.291
0.060	216.323	308.177	12.998
0.062	216.611	4470.830	13.901
<i>b</i> = 0.03			
0.010	2.652	−4.230	5.774
0.012	3.010	−10.390	5.861
0.020	5.117	75.489	6.244
0.030	12.753	75.721	6.854
0.040	20.243	76.118	7.729
0.050	275.248	78.217	9.119
0.060	277.955	302.607	12.564
0.062	278.211	4560.400	13.444
<i>b</i> = 0.05			
0.010	2.759	−4.0890	6.273
0.012	3.147	−10.4786	6.358
0.020	5.511	706.251	6.723
0.030	15.401	706.423	7.292
0.040	106.837	706.601	8.083
0.050	125.055	707.048	9.295
0.060	127.121	739.031	11.848
0.062	127.333	3491.830	12.688
<i>b</i> = 0.1			
0.010	2.947	−3.686	5.653
0.012	3.393	−10.048	5.751
0.020	6.317	114.000	6.125
0.030	24.130	114.204	6.662
0.040	92.917	114.502	7.390
0.050	99.406	115.878	8.480
0.060	100.803	289.511	10.679
0.062	100.961	4244.030	11.454

tremely sensitive to the approaches a value of 0.0.  $\mu_w \rightarrow \infty$ . According to that in Eq. 39 gives a h not yield satisfactory res

## RADICAL POLYMERIZATION

Unlike step growth polymerization, in chain reaction polymerization, the growing chain ends are called active centers. The active centers are monomer molecules to which the monomer molecules add to form the growing polymer chain.

The growth centers can be of two types: (1) in nature depending on the nature of the active centers, chain reaction polymerization can be coordination (or stereoregular) or free radical. Free radical polymerization is considerably more in nature than coordination polymerization.

Initiators for radical polymerization are two types of radicals:

1. Primary radicals,
2. Growing chains radicals and the n

The growing chain radical is known as propagating radical or between two propagating radicals; such species in the reaction mechanism are called radicals, growing chain radicals, growing chain radical polymerization kinetics—must be understood.

## Initiation

The molecules of initiator are broken down into free radicals by heat, light, or high-energy radiation. The free radicals are sensitive initiators such as azobisisobutyronitrile, which can be generated between a pair of molecules. During the reaction, an unpaired electron. During the reaction, a compound (called the active center) is formed. Redox initiators is a ferrous salt. Heat-sensitive initiators are

The homolytic decomposition of initiators is usually as

extremely sensitive to the closure approximation. It was observed earlier that as  $K$  approaches a value of 0.0625, for hexafunctional polymerization gelation would occur and  $\mu_w \rightarrow \infty$ . According to this table the moment closure in Eq. 41 gives finite  $\mu_{w\text{eq}}$  while that in Eq. 39 gives a high value. This implies that the empirical relation in Eq. 39 does not yield satisfactory results near the gel point.

## RADICAL POLYMERIZATION

Unlike step growth polymerization in which the reaction occurs between the functional groups, in chain reaction polymerization the monomer polymerizes in the presence of compounds called initiators. The initiator continually generates growth centers in the reaction mass, and monomer molecules are rapidly added. It is this sequential addition of monomer molecules to growing centers which differentiates chain reactions from step growth polymerization.

The growth centers can be ionic (cationic and anionic), free radical, or coordinational in nature depending on the kind of initiator system used. Based on the nature of the growth centers, chain reaction polymerization is further classified as radical, cationic, anionic, or coordination (or stereoregular) polymerization [75]. Radical polymerization is utilized considerably more in industry and the discussion in this section is confined to radical polymerization.

Initiators for radical polymerization generate free radicals in the reaction mass. There are two types of radicals present in the reaction mass during polymerization:

1. Primary radicals, which are generated by initiator molecules directly.
2. Growing chains radicals, which are generated by the reaction between the primary radicals and the monomer molecules.

The growing chain radicals keep adding monomer molecules sequentially; this type of reaction is known as propagation. Reaction between a primary radical and a polymer radical or between two polymeric radicals makes polymer radicals unreactive by destroying their radical nature; such reactions are called termination. There are thus five kinds of species in the reaction mass at any time: initiator molecules, monomer molecules, primary radicals, growing chain radicals, and terminated polymer molecules. In order to model radical polymerization kinetically, the various reactions—initiation, propagation, and termination—must be understood.

### Initiation

The molecules of initiator (denoted by  $I_2$ ) can generate radicals by a homolytic decomposition of covalent bonds on absorption of energy, which can be in the form of heat, light, or high-energy radiation, depending on the initiator employed. Commercially, heat-sensitive initiators such as azo or peroxide compounds are employed. Radicals could also be generated between a pair of compounds, called redox initiators, one of which contains an unpaired electron. During the initiation, the unpaired electron is transferred to the other compound (called the acceptor), which undergoes bond dissociation. An example of redox initiators is a ferrous salt with hydrogen peroxide. In this section, however, only heat-sensitive initiators are discussed primarily because of their extensive use in industry.

The homolytic decomposition of initiator molecules can be represented schematically as



where  $I_2$  is the initiator molecule and  $I$ , the primary radical. The rate of production of primary radicals,  $r_i'$  according to Eq. 46, is

$$r_i' = 2k_1[I_2] \quad (47)$$

where  $[I_2]$  is the concentration of the initiator in the system at any time.

The primary radicals,  $I$ , combine with a monomer molecules,  $M$ , according to the schematic reaction



where  $P_1$  is the polymer chain radical having one monomeric unit on it and  $k_1$  is the rate constant of reaction. The rate of production,  $r_i$ , of the polymer radicals,  $P_1$ , can be written as

$$r_i = k_1[I][M] \quad (49)$$

where  $[I]$  and  $[M]$  are the concentrations of the primary radical and the monomer in the reaction mass, respectively.

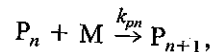
Equations 47 and 49 imply that all the radicals generated by the homolytic decomposition of initiator molecules are used in generating the polymer chain radicals and no primary radicals are wasted by any other reaction. This is not true in reality and an initiator efficiency is defined to take care of the waste of primary radicals. The initiator efficiency,  $f$ , is the fraction of the total primary radicals produced by reaction 46 which are used in generating polymer radicals by reaction 48. Thus the rate of generation of polymer radicals is given by

$$r_i = 2fk_1[I_2] \quad (50)$$

Sometimes a solvent is added to the monomer for better temperature control. This has been shown to affect the initiator efficiency and is explained in terms of the cage theory [76, 77]. On supplying energy to initiator molecules, cleavage of a covalent bond occurs as shown in Eq. 46. According to this theory, the two dissociated fragments are surrounded by the reaction mass, which forms a sort of cage around them. The two fragments stay inside the cage for a finite amount of time during which they can recombine to give back the initiator molecule. The fragments that do not recombine diffuse, and the separated fragments are called primary radicals. If the monomer molecule is highly reactive, it can also react with a fragment inside a cage. The characteristics of the reaction medium determine how long the dissociated fragments stay inside the cage and they also affect the initiator efficiency. It is therefore expected that, if all other conditions are equal, a more viscous reaction mass would lead to a lower initiator efficiency.

### Propagation Reaction

The propagation reaction is defined as the addition of monomer molecules to the growing polymer radicals. In the reaction mass there are polymer radicals of all possible sizes. In general, a polymer radical,  $P_n$ , indicates that there are  $n$  monomeric units joined together by covalent bonds in the chain radical. The propagation reaction can be written schematically as

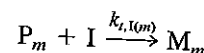
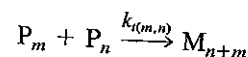


where  $k_{pn}$  is the rate constant. In general this would depend on increasing mathematical order. As a good first approximation, in the case of polymer radicals,

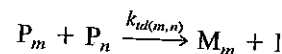
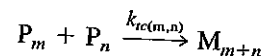
$$k_{p1} = k_{p2} = k_{p3} = \dots$$

### Termination of Polymer Radicals

The termination reaction can occur only when a primary radical. The formation of these reactions can be written as



where  $m, n = 1, 2, 3, \dots$ . In the absence of any further propagation reaction, the chains can be formed either by termination, two chain radicals combine to form one chain radical, or by disproportionation, one chain radical becomes inactive. These two reactions can be written as



where  $k_{tc(m,n)}$  and  $k_{td(m,n)}$  are the rate constants for termination and disproportionation, respectively. It is to be noted that to hold: all the rate constants are equal, i.e.,

$$k_{tc(m,n)} = k'_{tc} \quad \text{for } m \neq n$$

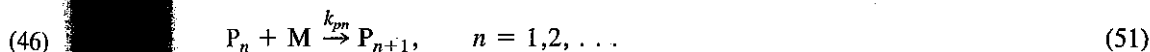
$$k_{td(m,n)} = k'_{td} \quad \text{for } m \neq n$$

$$k_{tc(m,n)} = \frac{k'_{tc}}{2}$$

$$k_{td(m,n)} = \frac{k'_{td}}{2} \quad \text{for all } m, n$$

Various reactions occurring in the system [1, 3]. The intermediate species, etc., and the mole balance equation for a batch reactor can be written as

$$\frac{d[I_2]}{dt} = k_1[I_2]$$



where  $k_{pn}$  is the rate constant for the reaction between  $P_n$  and a monomer molecule,  $M$ . In general this would depend on the size of the chain radical. It is not difficult to foresee the increasing mathematical complexity resulting from the multiplicity of the rate constants. As a good first approximation, the principle of equal reactivity is assumed to be valid even in the case of polymer radicals, which means that

$$k_{p1} = k_{p2} = k_{p3} = \dots = k_{pn} = k_p \quad (52)$$

### Termination of Polymer Radicals

The termination reaction is the one in which polymer chain radicals are destroyed. This can occur only when a polymer radical reacts with another polymer radical or with a primary radical. The former is called the mutual termination and the latter primary termination. These reactions can be written as



where  $m, n = 1, 2, 3, \dots$ .  $M_{n+m}$  signifies a dead polymer chain, i.e., it cannot undergo any further propagation reaction. In the case of mutual termination the inactive polymer chains can be formed either by combination or by disproportionation. In combination termination, two chain radicals just combine to give an inactive chain, whereas in disproportionation, one chain radical gives up an electron to the other and both chains become inactive. These two types of termination can be represented by



where  $k_{tc(m,n)}$  and  $k_{td(m,n)}$  are the rate constants for termination by combination and disproportionation, respectively. Once again, the principle of equal reactivity is assumed to hold: all the rate constants are independent of the chain lengths of the polymer radicals, i.e.,

$$k_{tc(m,n)} = k'_{tc} \quad (55a)$$

$$k_{td(m,n)} = k'_{td} \quad \text{for } m \neq n \quad (55b)$$

$$k_{tc(m,n)} = \frac{k'_{tc}}{2} \quad (55c)$$

$$k_{td(m,n)} = \frac{k'_{td}}{2} \quad \text{for all } m = n \quad (55d)$$

Various reactions occurring in radical polymerization are summarized in the Table 7 [1, 3]. The intermediate species present at the time in the reaction mass are  $I, P_1, P_2, P_3$ , etc., and the mole balance equations for each of these and the initiator molecule  $I_2$  in a batch reactor can be written as

$$\frac{d[I_2]}{dt} = k_1[I_2] \quad (56a)$$

$$\frac{d[I]}{dt} = 2fk_1[I_2] - k_1[I][M] - k_{tp}[I] \sum_{m=1}^{\infty} [P_m] \quad (56b)$$

$$\begin{aligned} \frac{d[P_1]}{dt} = & k_1[I][M] - k_p[P_1][M] - k_{tp}[P_1][I] \\ & - k'_t\{[P_1]^2 + [P_1][P_2] + [P_1][P_3] + \dots\} \end{aligned} \quad (56c)$$

$$\begin{aligned} \frac{d[P_n]}{dt} = & k_p[M][P_{n-1}] - k_p[M][P_n] - k_{tp}[P_n][I] \\ & - k'_t\{[P_n][P_1] + [P_n][P_2] + \dots + [P_n]^2 + \dots\} \end{aligned} \quad (56d)$$

where

$$k'_t = k'_{tc} + k'_{td} \quad (56e)$$

If  $[P]$  is defined as the total concentration of polymer radicals in the reaction mass, then

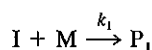
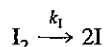
$$[P] = [P_1] + [P_2] + \dots = \sum_{n=1}^{\infty} [P_n] \quad (57)$$

and Eqs. 56c, d, and e can be added to give the rate of production of  $[P]$  as

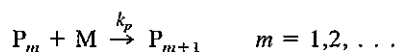
$$\frac{d[P]}{dt} = \frac{d \sum_{n=1}^{\infty} [P_n]}{dt} = k_1[I][M] - k_{tp}[I][P] - k'_t[P]^2 \quad (58)$$

**Table 7** Reactions Occurring in Radical Polymerization

Initiation:



Propagation:

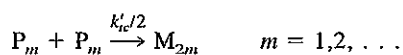
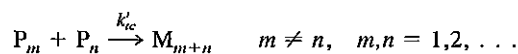


Termination:

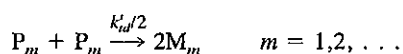
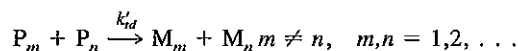
Primary:



Combination:



Disproportionation:



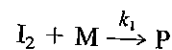
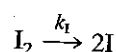
The corresponding relation

$$\frac{d[I_2]}{dt} = -k_1[I_2]$$

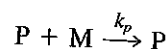
$$\frac{d[I]}{dt} = 2fk_1[I_2] - k_1[I]$$

The study of Eqs. 58 and 59 can be derived from the mole balance equation.

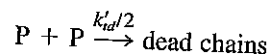
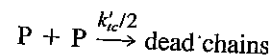
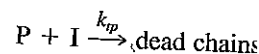
Initiation:



Propagation:



Termination:



The kinetic equivalence established. The replacement of each molecular species in the equations by its equivalent is analogous to simplification of growth polymerization by the use of the kinetic equivalence. The mole balance equation in Eqs. 58 and 59. Since the rate of termination is generally much higher than the rate of propagation,  $k_1[M] \gg k_p[P]$

Eq. 59b can be written as

$$\frac{d[I]}{dt} \approx 2fk_1[I_2] - k_1[I][M]$$

Also, in radical polymerization, and as soon as a primary radical is formed, it reacts with monomer. Thus the concentration of monomer is much higher than the concentration of polymer radicals,  $[M] \gg [P] \gg [I]$



(56b)

The corresponding relation for the initiation steps can be written from Eqs. 56a and b as

$$\frac{d[I_2]}{dt} = -k_i[I_2] \quad (59)$$

(56c)

$$\frac{d[I]}{dt} = 2fk_i[I_2] - k_1[I][M] - k_{ip}[I][P] \quad (59b)$$

(56d)

The study of Eqs. 58 and 59 reveals that these involve only [P]. An identical set of equations can be derived from the following simplified mechanism of the radical polymerization.

(56e)

Initiation:



icals in the reaction mass, then

(57)



Propagation:

duction of [P] as

(58)



Termination:



The kinetic equivalence of the mechanisms given in Table 7 and Eqs. 60 is thus established. The replacement of a complex series of equations given in Table 7, where each molecular species in the reaction mass is distinguished by the far simpler Eqs. 60, is analogous to simplification of the complex reactions involving individual species in step growth polymerization by the reaction between reactive groups. Indeed, both these simplifications are a direct consequence of the equal reactivity hypothesis.

The mole balance equations can be simplified even beyond the simplification achieved in Eqs. 58 and 59. Since the number of monomer molecules in the reaction mass is generally much higher than the number of polymer radicals,

$$k_1[M] \gg k_{ip}[P] \quad (61)$$

Eq. 59b can be written as

$$\frac{d[I]}{dt} \cong 2fk_i[I_2] - k_1[I][M] \quad (62)$$

Also, in radical polymerization the slowest reaction is the dissociation of initiator molecules, and as soon as a primary radical is produced, it is consumed by reactions b and c of Eqs. 60. Thus the concentration of I is expected to be much less than that of P, i.e.,

$$[M] \gg [P] \gg [I] \quad (63)$$

and Eq. 58 can be rewritten as

$$\frac{d[P]}{dt} = k_1[I][M] - k'_t[P]^2 \quad (64)$$

Equations 62 and 64 imply that the primary termination step, Eq. 60d, can be neglected in the kinetic mechanism.

The rate of monomer consumption  $r_p$  for radical polymerization can now be derived from Eqs. 60b and c and approximated as

$$r_p \approx k_p[P][M] \quad (65)$$

To find the total concentration of chain radicals, P, in the reaction mass, the steady-state approximation is used [78]. From Eq. 62,

$$\frac{d[I]}{dt} = 2fk_1[I_2] - k_1[M][I] = 0 \quad (66)$$

$$[I] = \frac{2fk_1[I_2]}{k_1[M]} \quad (67)$$

Similarly, from Eq. 64,

$$\frac{d[P]}{dt} = k_1[M][I] - k'_t[P]^2 = 0 \quad (68)$$

and from Eqs. 67 and 67,

$$[P] = \frac{2fk_1[I_2]^{1/2}}{k'_t} \quad (69)$$

The rate of propagation after some induction time is thus given by

$$r_p = k_p \left\{ \frac{2fk_1[I_2]^{1/2}}{k'_t} \right\} [M] \quad (70)$$

### Average Molecular Weight in Radical Polymerization

Average molecular weight in radical polymerization can be found from the kinetic model, Eqs. 60, as follows. The kinetic chain length,  $\nu$ , is defined as the average number of monomer molecules reacting with a polymer chain radical during the latter's entire lifetime. This is the ratio of the rate of consumption of the monomer, to the rate of generation of polymer radicals,  $r_i$ :

$$\nu = \frac{r_p}{r_i} \quad (71)$$

From the steady-state approximation, the rate of initiation,  $r_i$ , should be equal to the rate of termination,  $r_t$ . Therefore,

$$\nu = \frac{r_p}{r_i} = \frac{k_p[M][P]}{k'_t[P]} = \frac{k_p[M]}{k'_t[P]} \quad (72)$$

On eliminating [P] with the help of Eq. 69,  $\nu$  is given by

$$\nu = \frac{k_p}{(2fk_1k'_t)^{1/2}} \frac{[M]}{[I_2]^{1/2}} \quad (73)$$

Equation 73 shows that the concentration. This is expected produced.

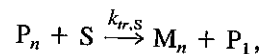
The quantity that is of interest  $\nu$  because  $\mu_n$  gives the average  $\nu$  because  $\nu$  gives the average  $\nu$ . To be able to find the exact  $\nu$  must be carefully analyzed. combination, then each of the termination occurs only by  $\nu$  would consist of  $\nu$  monomer then

$$\mu_n = \alpha \nu$$

where  $\alpha$  would be between 1

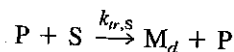
As the initiator concentration but  $\nu$ , and therefore  $\mu_n$ , goes tion is one way of monitoring

Another method for controlling transfer agent. The polymer capacity to add any further acquiring radical character in molecules like any other group represented schematically as



where S is a molecule of the t

Equation 75 should be added carried out with a transfer agent in the reaction mass, it is not other once again, and Eq. 75 c



Since this reaction does not reaction mass, from Eq. 65 it  $r_p$ . However, the kinetic chain  $k_{tr,S}$  and [S]. Equation 72 can agents:

$$\nu = \frac{r_p}{k'_t[P]^2 + k_{tr,S}[P][S]}$$

or on taking the reciprocal

$$\frac{1}{\nu} = \frac{k_{tr,S}[S]}{k_p[M]} + \frac{(2fk_1k'_t)^{1/2}}{k_p} \frac{[I_2]^{1/2}}{[M]}$$

Equation 78 predicts a decrease

Equation 73 shows that the kinetic chain length reduces with increasing initiator concentration. This is expected since an increase in  $[I_2]$  would lead to more chains being produced.

The quantity that is of interest is the average chain length,  $\mu_n$ . This is directly related to  $\nu$  because  $\mu_n$  gives the average number of monomer molecules per dead polymer chain whereas  $\nu$  gives the average number of monomer molecules per growing polymer radical. To be able to find the exact relationships between the two, the mechanism of termination must be carefully analyzed. If the termination of polymer radicals occurs only by combination, then each of the dead chains would consist of  $2\nu$  monomer molecules. If termination occurs only by disproportionation, each of the inactive polymer molecules would consist of  $\nu$  monomer molecules. If termination occurs by both these mechanisms, then

$$\mu_n = \alpha \nu \quad (74)$$

where  $\alpha$  would be between 1 and 2.

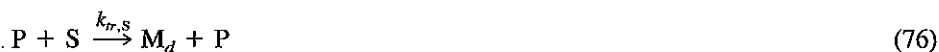
As the initiator concentration is increased, the rate of polymerization goes up (Eq. 70), but  $\nu$ , and therefore  $\mu_n$ , goes down (Eq. 73). Therefore, control of the initiator concentration is one way of monitoring the molecular weight of the polymer.

Another method for controlling the molecular weight of the polymer is the use of a transfer agent. The polymer chain radicals react with the transfer agent and lose the capacity to add any further monomer molecules, the molecule of the transfer agent acquiring radical character in this process. The latter can grow by adding monomer molecules like any other growing chain in the reaction mass. The transfer reaction is represented schematically as



where S is a molecule of the transfer agent.

Equation 75 should be added to the kinetic model if radical polymerization is being carried out with a transfer agent. Since the transfer reaction occurs with equal likelihood in the reaction mass, it is not necessary to distinguish chain radicals kinetically from each other once again, and Eq. 75 can be included in the following form in Eqs. 60:



Since this reaction does not reduce or increase the total number of chain radicals in the reaction mass, from Eq. 65 it follows that the presence of a transfer agent does not affect  $r_p$ . However, the kinetic chain length,  $\nu$ , changes drastically depending on the value of  $k_{tr,S}$  and  $[S]$ . Equation 72 can easily be modified to account for the presence of transfer agents:

$$\nu = \frac{r_p}{k_t'[P]^2 + k_{tr,S}[P][S]} \quad (77)$$

or on taking the reciprocal

$$\frac{1}{\nu} = \frac{k_{tr,S}[S]}{k_p[M]} + \frac{(2fk_t k_t')^{1/2}}{k_p} \frac{[I_2]^{1/2}}{[M]} \quad (78)$$

Equation 78 predicts a decrease in  $\mu_n$  with increasing concentration of the transfer agent.

Chain transfer reactions occur quite commonly in radical polymerization with initiator as well as monomer as follows:

With initiator:



With monomer:



These reactions can be similarly incorporated into the kinetic model and the average chain lengths can be found to be

$$\frac{1}{\alpha \mu_n} = C_M + C_S \frac{[S]}{[M]} + \frac{k_t}{k_p^2} \frac{r_p}{[M]^2} + C_1 \left( \frac{k'_t}{2fk_p^2 k_1} \right) \frac{r_p^2}{[M]^3} \quad (81)$$

where

$$C_M = \frac{k_{tr,M}}{k_p} \quad (82a)$$

$$C_1 = \frac{k_{tr,I_2}}{k_p} \quad (82b)$$

$$C_S = \frac{k_{tr,S}}{k_p} \quad (82c)$$

### Gel Effect in Radical Polymerization

The considerable increase in the rate of polymerization (as shown in Fig. 12 [75]) and the average chain length,  $\mu_n$  (Figure 13 [80]) is a phenomenon common to all monomers

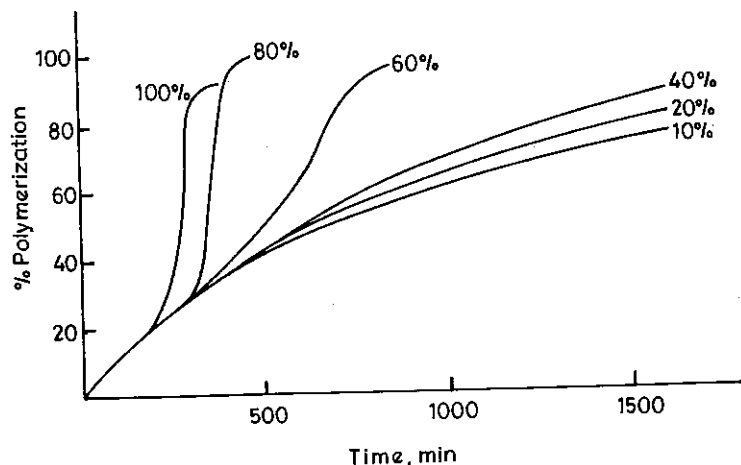


Figure 12 Polymerization of methyl methacrylate at 50°C with benzoyl peroxide initiator at various monomer concentrations (benzene as diluent).

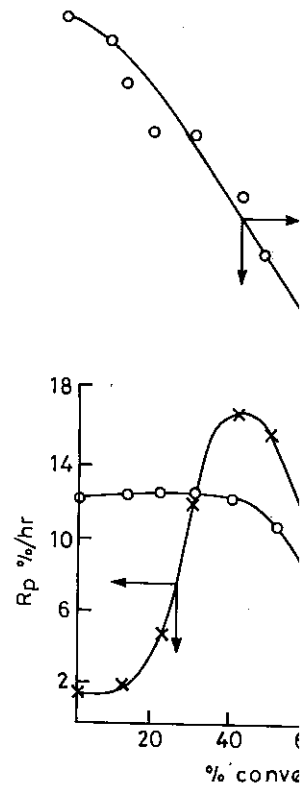
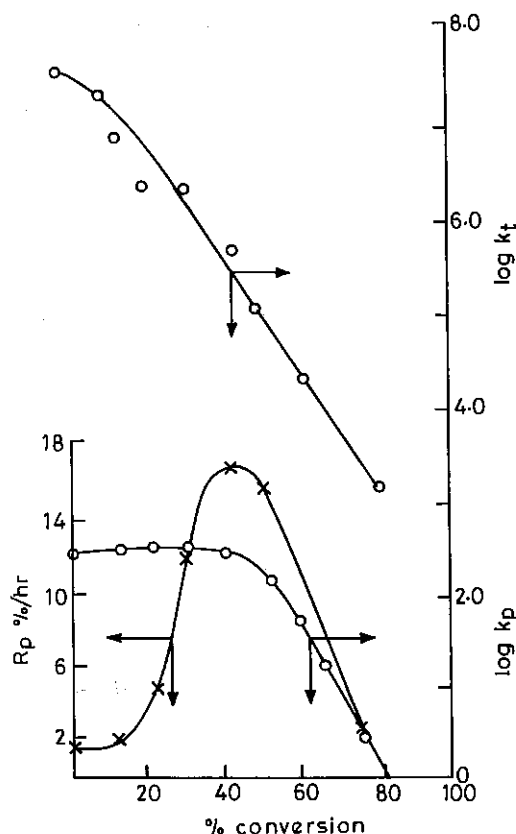


Figure 13 Average molecular weight of methyl methacrylate at 60°C and 0.004 M initiator (Washington.)

undergoing radical polymerization or gel effect. This has been observed in the fall in values of the rate of polymerization,  $r_p$ , at high conversions (Figure 14). It is also seen that the rate of polymerization is considerably faster than  $k_p$ , and the termination step involves the proximity of other radicals. Once the radicals undergo segmental diffusion occurs because the segmental motion of the reaction mass. On the other hand, a small molecule (i.e., monomer) undergoes segmental diffusion involve higher conversions.

During the course of free radical polymerization, the molecular weight changes in several regimes of changes consisting of dissolved, non-



**Figure 13** Average molecular weight as a function of conversion in the polymerization of methyl methacrylate at 60°C and 0.0045 mol % initiator. (Reprinted from Ref. 83, with permission of ACS, Washington.)

undergoing radical polymerization at low temperatures and is called the autoacceleration, or gel effect. This has been a subject of several studies [81–95] and has been attributed to the fall in values of the rate constants,  $k_p$  and  $k_t$ , as shown for methyl methacrylate in Figure 14. It is also seen that the rate constant  $k_t$  is affected first and falls in magnitude considerably faster than  $k_p$ . The large fall in  $k_t$  can be explained by observing that the termination step involves the diffusion of two polymer molecules from the bulk to each other's proximity. Once the proximate pair has been formed, the radical segments must undergo segmental diffusion before the termination reaction can occur. The fall in  $k_t$  occurs because the segmental diffusion becomes sluggish with the increase in the viscosity of the reaction mass. On the other hand, the propagation reaction involves the diffusion of a small molecule (i.e., monomer) from the bulk to the radical segment. There is little segmental diffusion involved in this step, thus leaving  $k_p$  unaffected up to considerably higher conversions.

During the course of free radical polymerization from the bulk monomer to complete or limiting conversion, the movement of polymer radicals toward each other goes through several regimes of changes. To demonstrate this, attention is focused on a solution consisting of dissolved, nonreacting polymer molecules. When the solution is very dilute,

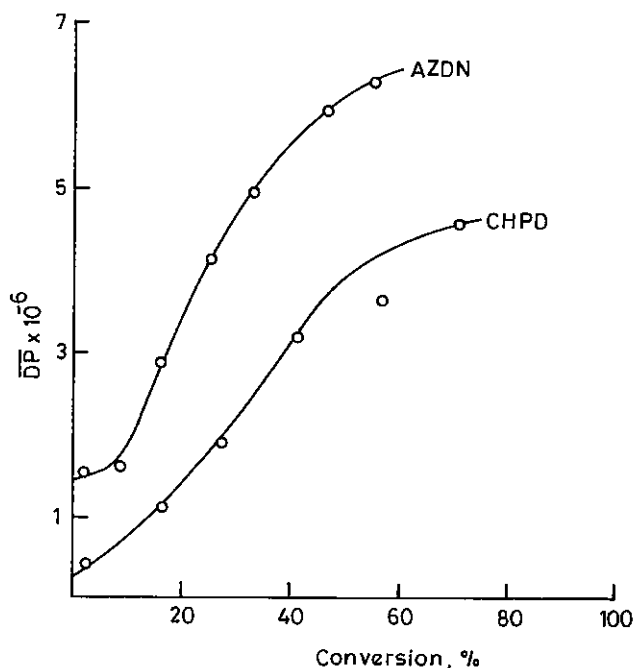


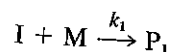
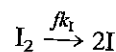
Figure 14 Bulk polymerization 25°C with AzDN initiator. The rate of initiation is  $8.36 \times 10^{-9}$  moles L sec<sup>-1</sup>.

the polymer molecules exist in a highly coiled state and they behave like hydrodynamic spheres. In this regime, polymer molecules can undergo translational motion easily and the overall diffusion is completely governed by polymer-solvent interactions. As the polymer concentration is increased (say beyond a critical conversion  $C^*$ ), the translational motion of molecule begins to be affected by the presence of other molecules. This effect, which was absent earlier, constitutes the second regime. On increasing the concentration of the polymer still further (say beyond  $C^{**}$ ), in addition to the intermolecular interactions in translational motion, polymer chains begin to impose topological constraints upon the motion of surrounding molecules due to their long-chain nature. In other words, polymer molecules begin to be entangled. DeGennes modeled the motion of polymer chains in this regime through a "tube" defined by the points of entanglement. A polymer molecule can move through this only by a snakelike wriggling motion along its length; this mode of motion is sometimes called reptation. Finally, at very high concentrations (say beyond  $C^{***}$ ), polymer chains begin to exert direct friction upon each other. The values of  $C^*$ ,  $C^{**}$ , and  $C^{***}$  have been experimentally shown to depend on the molecular weight of the polymer.

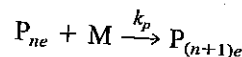
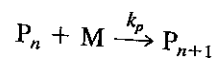
To demonstrate the correspondence between the polymer solvent system described above and free radical polymerization, Turner [90] and Driscoll's group [82, 91-93] demonstrated that gelation starts at the polymer concentration of  $C^{**}$ . In fact, it has been shown that  $k_t$  changes continuously as the polymerization progresses [89, 95], first increasing slightly but subsequently reducing drastically at higher conversions. Tulig and Tirrell [89, 95] have argued, based on their experimental and theoretical analysis, that similar regimes for  $k_t$  must exist in the entire range of conversion.

Based upon the foregoing Cardenas and O'Driscoll [82] exist in the reaction mass.  $P_{ne}$  and therefore have low second population (denoted  $P_e$ ) grows in chain length beyond and its termination rate constant,  $k_p$ , is not affected then by represented as follows:

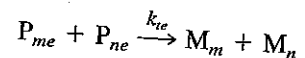
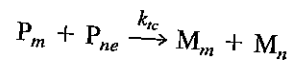
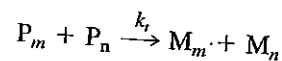
Initiation:



Propagation:



Termination:



In the above scheme, the reaction has been assumed to occur with rate equations for the various radicals above, and for batch reactors

$$\frac{d[P_1]}{dt} = 2fk_i[I_2] - \{k_p[M]P_1\}$$

$$\frac{d[P_n]}{dt} = [M][P_{n-1}] - \{k_p[M]P_n\}$$

$$\frac{d[P_{ne}]}{dt} = k_p[M][P_{(n-1)e}] - \{k_p[M]P_{ne}\}$$

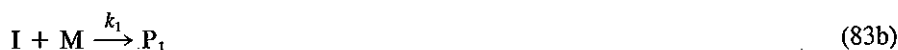
where

$$[P] = \sum_{n=1}^{n_c} [P_n]$$

$$[P_e] = \sum_{n=n_c+1}^{\infty} [P_{ne}]$$

Based upon the foregoing physical picture of the gel effect, a model was proposed by Cardenas and O'Driscoll [82, 91, 92] in which two populations of radicals are assumed to exist in the reaction mass. The first are those which are physically entangled (denoted by  $P_{ne}$ ) and therefore have lower termination rate constant ( $k_{te}$ ), compared to that ( $k_t$ ) of the second population (denoted by  $P_n$ ), which are unentangled. Whenever a polymer radical grows in chain length beyond a critical value  $n_c$ , it is assumed that it becomes entangled and its termination rate constant falls from  $k_t$  to  $k_{te}$ . If it is assumed that the propagation rate constant,  $k_p$ , is not affected, the overall mechanism of radical polymerization can then be represented as follows:

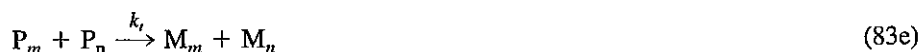
Initiation:



Propagation:



Termination:



In the above scheme, the reaction between the entangled and the unentangled radicals has been assumed to occur with rate constant  $k_{te}$  lying between  $k_t$  and  $k_{te}$ . The mole balance equations for the various radicals can be easily written from the kinetic mechanism given above, and for batch reactors

$$\frac{d[P_1]}{dt} = 2fk_1[I_2] - \{k_p[M] + 2k_t[P] + 2k_{te}[P_e]\}[P_1] \quad (84)$$

$$\frac{d[P_n]}{dt} = [M][P_{n-1}] - \{k_p[M] + 2k_t[P] + 2k_{te}[P_e]\}[P_n], \quad 2 \leq n \leq n_c \quad (85)$$

$$\frac{d[P_{ne}]}{dt} = k_p[M][P_{(n-1)e}] - \{k_p[M] + 2k_{te}[P] + 2k_{te}[P_e]\}[P_{ne}], \quad n_e > n_c \quad (86)$$

where

$$[P] = \sum_{n=1}^{n_c} [P_n] \quad (87a)$$

$$[P_e] = \sum_{n=n_c+1}^{\infty} [P_n] \quad (87b)$$

rate of initiation is  $8.36 \times 10^{-9}$

they behave like hydrodynamic translational motion easily and solvent interactions. As the conversion ( $C^*$ ), the translational motion of other molecules. This effect, in increasing the concentration of the intermolecular interaction topological constraints of chain nature. In other words, hindered the motion of polymer radicals of entanglement. A polymer radical, sliding motion along its length; at very high concentrations friction upon each other. The rate is known to depend on the molecu-

mer solvent system described by O'Driscoll's group [82, 91-93] in terms of  $C^{**}$ . In fact, it has been shown that at higher conversions, Tulig and O'Driscoll's theoretical analysis, that

Since the total reaction time is usually much larger than the individual radical lifetime, the steady-state approximation can be assumed to valid here. On summing Eqs. 84 and 85 for values of  $n$  up to  $n_c$ , one gets

$$2fk_1[I_2] + k_p[M] \sum_{n=2}^{\infty} [P_{n-1}] - \{k_p[M] + 2k_t[P] + 2k_{tc}[P_e]\} \sum_{n=1}^{\infty} [P_n] = \frac{d[P]}{dt} = 0 \quad (88)$$

or

$$2fk_1[I_2] - \{2k_t[P] + 2k_{tc}[P_e]\}[P] = k_p[M][P_{nc}] \quad (89)$$

It is assumed that  $k_{tc}$  is the geometric mean of  $k_t$  and  $k_{te}$ , i.e.,

$$k_{tc} = (k_t k_{te})^{1/2} = \delta k_t \quad (90)$$

where

$$\delta = \left( \frac{k_{te}}{k_t} \right)^{1/2} \quad (91)$$

With the help of Eq. 90, Eq. 89 is simplified to

$$2fk_1[I_2] - 2k_t\{[P] + \delta[P_e]\}[P] = k_p[M][P_{nc}] \quad (92)$$

Similarly, Eq. 85 is added for all values of  $n$  above  $n_c$  assuming the steady-state approximation is valid. On doing this, the following relation is obtained:

$$k_p[M] \sum_{n=n_c+1}^{\infty} [P_{(n-1)e}] - \{k_p[M] + 2k_{tc}[P] + 2k_{te}[P_e]\} \sum_{n=n_c+1}^{\infty} [P_{ne}] = \frac{d[P_e]}{dt} = 0 \quad (93)$$

which simplifies to

$$2\delta k_t\{[P] + \delta[P_e]\} = k_p[M][P_{nc}] \quad (94)$$

Equating the left-hand sides of Eqs. 92 and 94,

$$[P] + \delta[P_e] = \left\{ \frac{fk_1[I_2]}{k_t} \right\}^{1/2} \quad (95)$$

It is now necessary to define the probability of propagation to find the distribution of  $P_n$ . After a polymer chain radical is formed by the reaction between a primary radical and a monomer molecule, it can either propagate by reaction 83c and d or be terminated by transfer or mutual termination reactions 83e, f, and g. Therefore, the probability of propagation,  $\beta$ , for chain length less than  $n_c$  is found as

$$\beta = \frac{k_p[M]}{k_p[M] + 2k_t[P] + 2k_{tc}[P_e]} = \frac{1}{1 + \{k_t fk_1[I_2]/k_p^2[M]^2\}^{1/2}} \quad (96)$$

where the transfer reactions have been neglected. Under the steady-state approximation,  $d[P_n]/dt$  is set equal to zero in Eq. 85. It is recognized that  $P_n$  is formed only when there is a propagation reaction with  $P_{n-1}$ , or

$$[P_n] = \beta[P_{n-1}] \quad \text{for}$$

Similarly, from the steady-

$$[P_1] = \frac{2fk_1[I_2]}{k_p[M]}$$

With the help of Eqs. 97 and

$$[P_n] = \beta^n \frac{2fk_1[I_2]}{k_p[M]}$$

It is observed that  $\beta$  is approximated by  $(\beta - 1)/\beta$

$$\beta^n = \exp(n \ln \beta) = \exp$$

where

$$\frac{1}{\nu} = 2 \left\{ \frac{k_t fk_1[I_2]}{k_p^2[M]^2} \right\}^{1/2}$$

and is the same as the kinetic from Eq. 99 and substituted

$$[P] = \left\{ \frac{fk_1[I_2]}{k_t} \right\}^{1/2} \left[ 1 - \right]$$

and

$$[P_e] = \left\{ \frac{fk_1[I_2]}{k_t} \right\}^{1/2} \exp(-$$

The rate of polymerization,  $r_p$

$$r_p = k_p[M]\{[P] + [P_e]\} =$$

The monomer conversion,  $x$ , concentration initially present dence time,  $[M]$ . This is given

$$x = \frac{[M]_0 - [M]}{[M]_0}$$

Equation 103 can now be writt

$$r_p = \frac{dx}{dt} = k_p(1-x) \left\{ \frac{fk_1[I_2]}{k_t} \right\}^{1/2}$$

To solve for the rate of poly determine  $\delta$  and  $n_c$ . From rheo age chain length  $\mu_{nc}$  and the vol

$$K_c = \mu_{nc} \phi_P$$



individual radical lifetime, the  
On summing Eqs. 84 and 85 for

$$\frac{d[P]}{dt} = 0 \quad (88)$$

$$(89)$$

$$(90)$$

$$(91)$$

$$(92)$$

ing the steady-state approxi-  
ined:

$$\sum_{n=n_c+1}^{\infty} [P_n] \quad (93)$$

$$(94)$$

$$(95)$$

on to find the distribution of  
between a primary radical and  
c and d or be terminated by  
therefore, the probability of

$$2^{1/2} \quad (96)$$

steady-state approximation,  
is formed only when there is

$$[P_n] = \beta[P_{n-1}] \quad \text{for } n \leq n_c \quad (97)$$

Similarly, from the steady-state approximation,  $d[P_1]/dt$  is equal to zero and Eq. 84 gives

$$[P_1] = \frac{2fk_1[I_2]}{k_p[M]} \quad (98)$$

With the help of Eqs. 97 and 98, one finds

$$[P_n] = \beta^n \frac{2fk_1[I_2]}{k_p[M]} \quad (99)$$

It is observed that  $\beta$  is a quantity close to unity, which implies that  $\ln \beta$  can be approximated by  $(\beta - 1)/\beta$  and the term  $\beta^n$  can be rewritten as

$$\beta^n = \exp(n \ln \beta) = \exp\left\{-n \frac{(-\beta + 1)}{\beta}\right\} = \exp\left(-\frac{n}{\nu}\right) \quad (100)$$

where

$$\frac{1}{\nu} = 2 \left\{ \frac{k_t f k_1 [I_2]}{k_p^2 [M]^2} \right\}^{1/2} \quad (101)$$

and is the same as the kinetic chain length defined in Eq. 73.  $[P_{n_c}]$  can now be calculated from Eq. 99 and substituted in Eqs. 94 and 95 to obtain

$$[P] = \left\{ \frac{fk_1[I_2]}{k_t} \right\}^{1/2} \left[ 1 - \exp\left(-\frac{n_c}{\nu}\right) \right] \quad (102a)$$

and

$$[P_e] = \left\{ \frac{fk_1[I_2]}{k_t} \right\}^{1/2} \exp\left(-\frac{n_c}{\nu}\right) \quad (102b)$$

The rate of polymerization,  $r_p$ , can now be determined as

$$r_p = k_p[M]\{[P] + [P_e]\} = k_p[M] \left\{ \frac{fk_1[I_2]}{k_t} \right\}^{1/2} \left[ 1 + \frac{1 - \delta}{\delta} \exp\left(-\frac{n_c}{\nu}\right) \right] \quad (103)$$

The monomer conversion,  $x$ , as radical polymerization is defined in terms of monomer concentration initially present in the reaction mass,  $[M]_0$ , and that at any reaction residence time,  $[M]$ . This is given by

$$x = \frac{[M]_0 - [M]}{[M]_0} \quad (104)$$

Equation 103 can now be written in terms of the monomer conversion,  $x$ , as

$$r_p = \frac{dx}{dt} = k_p(1 - x) \left\{ \frac{fk_1[I_2]}{k_t} \right\}^{1/2} \left[ 1 + \frac{1 - \delta}{\delta} \exp\left(-\frac{n_c}{\nu}\right) \right] \quad (105)$$

To solve for the rate of polymerization at a given conversion,  $x$ , it is necessary to determine  $\delta$  and  $n_c$ . From rheological studies, the relation between critical number average chain length  $\mu_{nc}$  and the volume fraction  $\phi_P$  of polymer present in solution is given by

$$K_c = \mu_{nc} \phi_P \quad (106)$$

$K_c$  is a constant which is (almost) independent of temperature but has different value for different polymers. In this equation  $\gamma$  is a constant that lies between 0.5 and 1.0, and it is found that the computed rate curves are relatively insensitive to the value of  $\gamma$  chosen. It is postulated that  $k_{te}$  is inversely proportional to the entanglement density  $d_e$  or

$$k_{te} = \frac{b}{d_e} \quad (107)$$

where  $b$  is a constant of proportionality and  $d_e$  is given by

$$d_e = a \left( \frac{\phi_p \mu_n}{K_c} \right) = d_e \theta \left( \frac{K_c}{\phi_p \mu_n} \right)^{1/2} \quad (108)$$

Equations 106–108 can be combined to give

$$d_{e0} = \left( \frac{b}{ak_t} \right)^{1/2} \quad (109)$$

To be able to solve average molecular weights, the mode of termination must be known. If it is assumed that termination occurs largely by the disproportionation mechanism,

$$\frac{d[M_n]}{dt} = \{2k_t[P] + 2k_{tc}[P_e]\}[P_n], \quad n \leq n_c \quad (110a)$$

$$\frac{d[M_n]}{dt} = \{2k_{tc}[P] + 2k_{te}[P_e]\}[P_{ne}], \quad n > n_c \quad (110b)$$

From Eqs. 110, it is possible to derive the zeroth ( $\lambda_0$ ), first ( $\lambda_1$ ), and second ( $\lambda_2$ ) moments of the inactive polymer chains as follows. For example,  $\lambda_2$  is given by

$$\frac{d\lambda_2}{dt} = \sum_{n=1}^{n_c} n^2 [P_n] \{2k_t[P] + 2k_{tc}[P_e]\} + \sum_{n=n_c+1}^{\infty} n^2 [P_{ne}] \{2k_{tc}[P] + 2k_{te}[P_e]\} \quad (111)$$

The moments of inactive polymers are thus related to the moments of the radicals, which can now be determined by Eqs. 84–86. Assuming the steady-state approximation, it is possible to derive from these relations the following:

$$\sum_{n=1}^{n_c} n^2 [P_n] = \frac{2fk_1[I_2] + k_p[M]\{2\sum_{n=1}^{n_c-1} n[P_n] + \sum_{n=1}^{n_c-1} [P_n] - n_c^2[P_{nc}]\}}{2k_t[P] + 2k_{tc}[P_e]} \quad (112a)$$

and

$$\sum_{n=n_c+1}^{\infty} n^2 [P_{ne}] = \frac{k_p[M]\{2\sum_{n=n_c}^{\infty} n[P_{ne}] + \sum_{n=n_c}^{\infty} [P_{ne}] + n_c^2[P_{nc}]\}}{2k_{tc}[P] + 2k_{te}[P_e]} \quad (112b)$$

Substituting these in Eq. 107, one obtains

$$\frac{d\lambda_2}{dt} = k_p[M]\{[P] + [P_e]\} + 2k_p[M] \sum_{n=1}^{\infty} n[P_n] \quad (113)$$

Similarly, it can be found that

$$\frac{d\lambda_0}{dt} = 2fk_1[I_2] \quad (114)$$

and

$$\frac{d\lambda_1}{dt} = k_p[M]\{[P] + [P_e]\}$$

Driscoll and coworkers [82] have solved these equations. 115, the number and weight 108,  $k_{te}$  and  $\gamma$  are computed. Conversion is obtained by integration of the polymerization given in Table 8. Experimental values of conversion theory is found to describe

Table 8 Parameters for the Polymerization of Methyl Methacrylate

Parameter	
$k_p (fk_1/k_t)^{1/2}$	7.5
$k_t/k_p^2$ (mol-sec L <sup>-1</sup> )	28
$k_t$ (sec <sup>-1</sup> )	3.5
$K_c$	8.97
$\alpha_p$	1.11
$1/f$	0.159

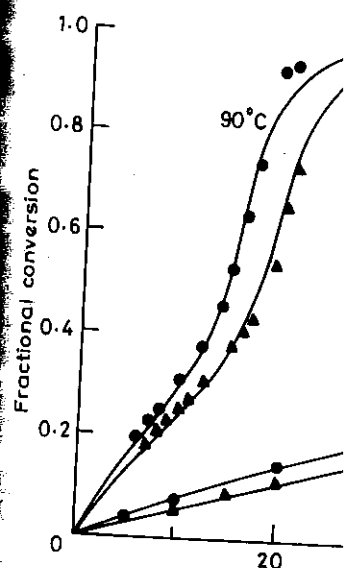


Figure 15 Experimental and predicted fractional conversion of methyl methacrylate  $[I_2]_0$  for (●) 0.01 M. John Wiley and Sons, New York.)

and

$$\frac{d\lambda_1}{dt} = k_p[M]\{[P] + [P_e]\} \quad (115)$$

Driscoll and coworkers [82] have treated  $K_c$  and  $d_{e0}$  in Eqs. 106 and 108 as parameters and have solved these equations simultaneously. From the moments calculated by Eqs. 113–115, the number and weight average molecular weights can be found. Using Eqs. 107 and 108,  $k_{te}$  and  $\gamma$  are computed. On substituting these in Eq. 103, the next incremental conversion is obtained by integration. For the set of parameters for methyl methacrylate polymerization given in Table 8, these equations have been integrated and compared with experimental values of conversion and molecular weights in Figures 15 and 16. The theory is found to describe the experimental data very well.

**Table 8** Parameters for the Radical Polymerization of Methyl Methacrylate

Parameter	Temperature (°C)	
	70	90
$k_p (fk_t/k_t)^{1/2}$	$7.5 \times 10^{-4}$	$3.8 \times 10^{-3}$
$k_t/k_p^2$ (mol-sec L <sup>-1</sup> )	28	16
$k_t$ (sec <sup>-1</sup> )	$3.5 \times 10^{-5}$	$5.0 \times 10^{-4}$
$K_c$	8.97	5.69
$\alpha_p$	$1.11 \times 10^{-1}$	$1.67 \times 10^{-1}$
$1/f$	0.1596	0.1731

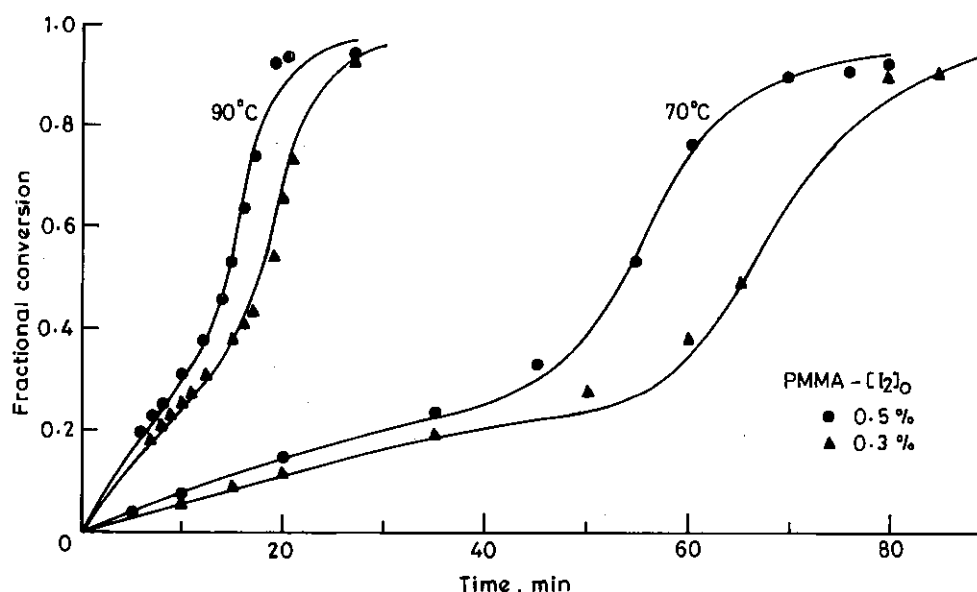


**Figure 15** Experimental and predicted values of conversion versus time of polymerization for methyl methacrylate  $[I_2]_0$  for (●) 0.5% and (▲) 0.3%. (Reprinted from Ref. 82, with permission of John Wiley and Sons, New York.)

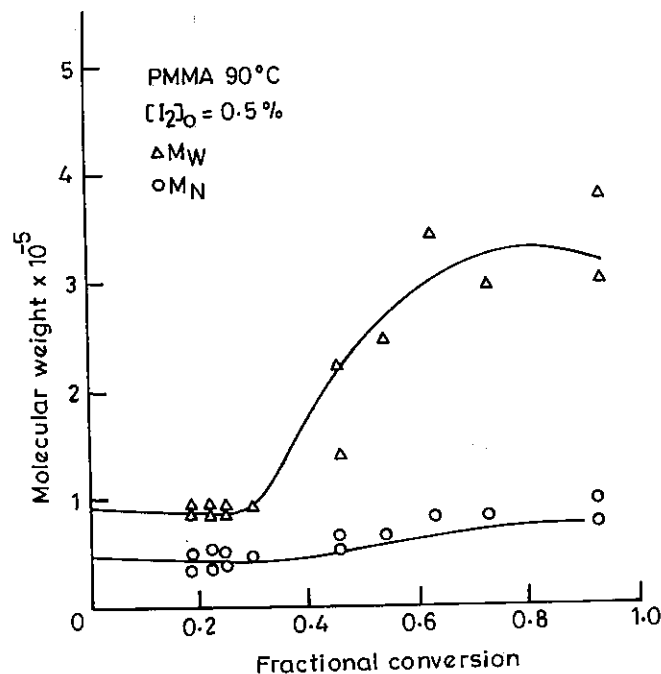


**Figure 16** Experimental and predicted values of molecular weight versus fractional conversion for methyl methacrylate with initiator concentration 0.5%. (Reprinted from Ref. 82, with permission of John Wiley and Sons, New York.)

### Temperature Effects in Radical Polymerization

In the initial stages (i.e., before the gel effect sets in) the temperature dependence of various rate constants can be expressed through the Arrhenius law:

$$k_1 = k_{10} e^{-E_1/RT}$$

$$k_p = k_{p0} e^{-E_p/RT}$$

$$k_t = k_{t0} e^{-E_t/RT}$$

In this representation,  $E_1$ ,  $E_p$ , and  $E_t$  are activation energies of the initiation, propagation, and termination steps respectively and are tabulated extensively in polymer handbooks [76]. The temperature dependence of  $r_p$  and  $\mu_n$  can be derived as

$$r_p = \frac{k_{p0} k_{t0}^{1/2}}{k_1^{1/2}} \exp\left(-\frac{E_p - E_t/2 + E_1/2}{RT}\right) \{f[I_2]^{1/2}[M]\}$$

$$\mu_n = \frac{k_{p0}}{2k_{t0}^{1/2} f^{1/2} k_1^{1/2}} \frac{[M]}{[I_2]^{1/2}} \exp\left(-\frac{E_p - E_t/2 - E_1/2}{RT}\right)$$

The activation energies are such that the overall polymerization for thermally dissociating initiator is exothermic, i.e.,  $(E_p - E_t/2 + E_1/2)$  is positive and rate increases with temperature. As opposed to this,  $\{E_p - E_t/2 - E_1/2\}$  is normally negative for such cases and  $\mu_n$  decreases with increasing temperature.

After the gel point sets in, the temperature dependence of  $k_p$  and  $k_t$  can be expressed by

$$k_p = k_{p0} \exp\left\{-E\left(\frac{1}{V_F} - \frac{1}{V_{Fc1}}\right)\right\}$$

$$k_t = k_{t0} \left(\frac{\mu_{wc}}{\mu_w}\right)^{1.75} \exp\left\{-A\left(\frac{1}{V_F} - \frac{1}{V_{Fc2}}\right)\right\}$$

where  $A$  and  $B$  are constants, whereas  $V_F$  is free volume fraction defined as

$$V_F = \{0.025 + \alpha_P(T - T_{gP})\} \frac{V_P}{V_T} + \{0.025 + \alpha_M(T - T_{gM})\} \frac{V_M}{V_T} + \{0.025 + \alpha_S(T - T_{gS})\} \frac{V_S}{V_T}$$

In these equations, subscripts P, M, and S denote polymer, monomer, and solvent respectively.  $T$  is the polymerization temperature,  $T_g$  is the glass transition temperature, and  $\alpha_g$  is the thermal expansion coefficient for the glassy state.  $V_{Fc1}$  is determined by the point where the propagation rate constant becomes diffusion controlled.  $V_T$  is the specific volume of the reaction mass.

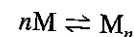
$$K_c = \mu_w^{0.5} \exp\left(\frac{A}{V_{Fc2}}\right)$$

$V_{Fc1}$  is determined by the point where the propagation rate constant becomes diffusion controlled.  $V_T$  is the specific volume of the reaction mass.

### REVERSIBLE RADICAL POLYMERIZATION

All polymerization reactions are reversible and have an equilibrium for a given temperature at which point the Gibbs free energy is zero. In the preceding section, the reaction steps were assumed to be irreversible in radical polymerization, which serve as good approximation only for low temperatures. Let us first consider the dynamic equilibrium for addition polymerization before presenting the kinetic model for reversible addition polymerization.

It is assumed that the formation of the polymer can be represented by



which states that  $n$  monomer molecules combine to form a polymer molecule of length  $n$ . The change in the Gibbs free energy  $\Delta G$  for this process is defined by

$$\begin{aligned} \Delta G &= \frac{1}{n} G_{\text{polymer}} - G_{\text{monomer}} \\ &= \left(\frac{1}{n} H_{\text{polymer}} - H_{\text{monomer}}\right) - T\left(\frac{1}{n} S_{\text{polymer}} - S_{\text{monomer}}\right) \\ &\triangleq \Delta H_p - T\Delta S_p \end{aligned}$$

where  $H$  and  $S$  represent enthalpy and entropy and  $\Delta H_p$  and  $\Delta S_p$  are the changes in enthalpy and entropy of polymerization per monomer unit, respectively.

Almost all addition polymerizations are exothermic. Moreover, polymerization is a process of joining monomer molecules by covalent bonds, something equivalent to

After the gel point sets in, the temperature dependence of  $k_p$  and  $k_t$  can be represented by

$$k_p = k_{p0} \exp \left\{ -E \left( \frac{1}{V_F} - \frac{1}{V_{Fc1}} \right) \right\}$$

$$k_t = k_{t0} \left( \frac{\mu_{wc}}{\mu_w} \right)^{1.75} \exp \left\{ -A \left( \frac{1}{V_F} - \frac{1}{V_{Fc2}} \right) \right\}$$

where  $A$  and  $B$  are constants, whereas  $V_F$  is free volume fraction defined as

$$V_F = \{0.025 + \alpha_P(T - T_{gP})\} \frac{V_P}{V_T} + \{0.025 + \alpha_M(T - T_{gM})\} \frac{V_M}{V_T}$$

$$+ \{0.025 + \alpha_S(T - T_{gS})\} \frac{V_S}{V_T}$$

In these equations, subscripts P, M, and S denote polymer, monomer, and solvent, respectively.  $T$  is the polymerization temperature,  $T_g$  is the glass transition temperature, and  $\alpha_g$  is the thermal expansion coefficient for the glassy state.  $V_{Fc2}$  is determined by the point where the gel point starts and is given by

$$K_c = \mu_w^{0.5} \exp \left( \frac{A}{V_{Fc2}} \right)$$

$V_{Fc1}$  is determined by the point where the propagation rate constant becomes diffusion controlled.  $V_T$  is the specific volume of the reaction mass.

## REVERSIBLE RADICAL POLYMERIZATION

All polymerization reactions are reversible and have an equilibrium for a given temperature at which point the Gibbs free energy is zero. In the preceding section, various reaction steps were assumed to be irreversible in radical polymerization, which would serve as good approximation only for low temperatures. Let us first consider the thermodynamic equilibrium for addition polymerization before presenting the kinetic model made for reversible addition polymerization.

It is assumed that the formation of the polymer can be represented by



which states that  $n$  monomer molecules combine to form a polymer molecule of chain length  $n$ . The change in the Gibbs free energy  $\Delta G$  for this process is defined by

$$\Delta G = \frac{1}{n} G_{\text{polymer}} - G_{\text{monomer}}$$

$$= \left( \frac{1}{n} H_{\text{polymer}} - H_{\text{monomer}} \right) - T \left( \frac{1}{n} S_{\text{polymer}} - S_{\text{monomer}} \right)$$

$$\triangleq \Delta H_p - T \Delta S_p \quad (117)$$

where  $H$  and  $S$  represent enthalpy and entropy and  $\Delta H_p$  and  $\Delta S_p$  are the changes in enthalpy and entropy of polymerization per monomer unit, respectively.

Almost all addition polymerizations are exothermic. Moreover, polymerization is the process of joining monomer molecules by covalent bonds, something equivalent to the

stringing of beads into a necklace, the final state being more ordered and consequently having a lower entropy. Thus  $\Delta S_p$  is always negative and is normally a large negative number, which cannot be neglected. Equation 117 therefore suggests that there is a ceiling temperature  $T_c$  at which the addition polymerization is at equilibrium (or  $\Delta G = 0$ ), i.e.,

$$T_c = \frac{\Delta H_p}{\Delta S_p} \quad (118)$$

For a given monomer concentration  $[M]$ ,  $\Delta S$  in this equation is equal to

$$\Delta S_p = \Delta S_p^0 + R \ln [M] \quad (119)$$

where  $\Delta S_p^0$  is the entropy change when the polymerization is carried out at standard state and is independent of  $[M]$ . The standard state of a liquid monomer is defined to be that at which monomer concentration is one molar at the temperature and pressure of the polymerization. If  $[M]_e$  is the monomer concentration at equilibrium, then

$$\ln [M]_e = \frac{\Delta H_p^0}{RT} - \frac{\Delta S_p^0}{R} \quad (120)$$

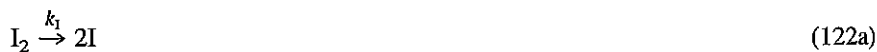
where  $\Delta H_p$  is the same as  $\Delta H_p^0$  by definition. As an example, for styrene being polymerized at 60°C,  $\Delta H_p^0$  is 16,700 cal mol<sup>-1</sup> and  $\Delta S^0$  25 cal mol-K<sup>-1</sup>.  $[M]_e$  for styrene at 60°C is given by

$$[M]_e = \exp \left\{ -\frac{16,700}{1.987(273 + 60)} + \frac{25}{1.987} \right\} = 3.7 \times 10^{-6} \text{ mol L}^{-1} \quad (121)$$

It is thus seen that at 60°C, polymerization would go to complete conversion. Polystyrene has a ceiling temperature of 670 K and as the polymerization temperature approaches this value, various reaction steps would become reversible and the analysis of the preceding section must be modified as follows.

In the irreversible mechanism of radical polymerization given in Table 7, the propagation step has considerably lower activation energies. Consequently, this step would become reversible first and the polymerization then can be represented as follows.

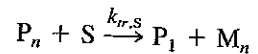
Initiation:



Propagation:



Termination:



Reactions in Eq. 124c and molecule or any transfer agent approximation is assumed to

$$\frac{d[P_1]}{dt} = k_1[M][I] - k_1[P_1]$$

$$+ k_{tr,S}[S] \sum_{n=2}^{\infty} [P_n]$$

$$\frac{d[P_2]}{dt} = k_p[M]\{[P_1] - [P_2]\}$$

$$- \{k_t[P] + k_{tr,M}[M]\}$$

$$\frac{d[P_n]}{dt} = k_p[M]\{[P_{n-1}] - [P_n]\}$$

$$- \{k_t[P] + k_{tr,M}[M]\}$$

where

$$k_t = k_{tc} + k_{td}$$

and

$$[P] = \sum_{i=1}^{\infty} [P_i]$$

On adding all relations from P

$$\frac{d\sum_{n=2}^{\infty} [P_n]}{dt} = 0 = k_p[M][P_1]$$

$$- \{k_t[P] + k_{tr,M}[M]\}$$

or

$$\sum_{n=2}^{\infty} [P_n] = \frac{k_p[M][P_1]}{k_t[P] + k_{tr,M}[M]}$$

$$- \frac{k_p[M][P_1]}{k_t[P] + k_{tr,M}[M]}$$

more ordered and consequently  $\Delta G^\ddagger$  is normally a large negative value. This suggests that there is a ceiling equilibrium (or  $\Delta G = 0$ ), i.e.,

(118)

on is equal to

(119)

is carried out at standard state monomer is defined to be that at pure and pressure of the polymer, then

(120)

ample, for styrene being polymerized at  $10^{-6} \text{ mol L}^{-1}$ .  $[M]_e$  for styrene at

(121)

complete conversion. Polystyrene at temperature approaches this value, the analysis of the preceding

given in Table 7, the propagation step would be represented as follows.

(122a)

(122b)

(123)

(124a)

(124b)



Reactions in Eq. 124c and d are transfer reactions, which can occur to a monomer molecule or any transfer agent that may be present in the reaction mass. If the steady-state approximation is assumed to hold, the mole balance for  $P_n$  is given by

$$\frac{d[P_1]}{dt} = k_1[M][I] - k_1[P_1] - k_p[M][P_1] + k'_p[P_2] + k_{tr,M}[M] \sum_{n=2}^{\infty} [P_n]$$

$$+ k_{tr,S}[S] \sum_{n=2}^{\infty} [P_n] - (k_{tc} + k_{td})[P_1][P] = 0$$

$$\begin{aligned} \frac{d[P_2]}{dt} &= k_p[M]\{[P_1] - [P_2]\} + k'_p\{[P_3] - [P_2]\} \\ &\quad - \{k_t[P] + k_{tr,M}[M] + k_{tr,S}[S]\}[P_2] = 0 \end{aligned}$$

$$\begin{aligned} &\vdots \\ &\vdots \\ &\vdots \end{aligned}$$

$$\begin{aligned} \frac{d[P_n]}{dt} &= k_p[M]\{[P_{n-1}] - [P_n]\} + k'_p\{[P_{n+1}] - [P_n]\} \\ &\quad - \{k_t[P] + k_{tr,M}[M] + k_{tr,S}[S]\}[P_n] = 0 \end{aligned}$$

$$\begin{aligned} &\vdots \\ &\vdots \\ &\vdots \end{aligned} \quad (125)$$

where

$$k_t = k_{tc} + k_{td} \quad (126a)$$

and

$$[P] = \sum_{i=1}^{\infty} [P_i] \quad (126b)$$

On adding all relations from  $P_2$  on, one gets

$$\begin{aligned} \frac{d\sum_{n=2}^{\infty} [P_n]}{dt} &= 0 = k_p[M][P_1] - k'_p[P_2] \\ &\quad - \{k_t[P] + k_{tr,M}[M] + k_{tr,S}[S]\} \sum_{n=2}^{\infty} [P_n] \end{aligned} \quad (127)$$

or

$$\begin{aligned} \sum_{n=2}^{\infty} [P_n] &= \frac{k_p[M]}{k_t[P] + k_{tr,M}[M] + k_{tr,S}[S]} [P_1] \\ &\quad - \frac{k'_p}{k_t[P] + k_{tr,M}[M] + k_{tr,S}[S]} [P_2] \end{aligned} \quad (128)$$

Substituting this in the balance for  $P_1$ , one has

$$\frac{d[P_1]}{dt} = k_1[M][I] - k'_1[P_1] + k_{tr,S}[S][P] + k_{tr,M}[M][P] + k'_p[P_2] \quad (129)$$

Balance for  $[I]$  combined with the steady-state hypothesis yields

$$\frac{d[I]}{dt} = 0 - 2fk_1[I_2] + k'_1[P_1] - k_1[M][I] = 0 \quad (130)$$

On adding all balance relations, one obtains  $[P]$  as

$$\frac{d[P]}{dt} = 0 = k_1[M][I] - k_1[P_1] - k_t[P]^2 \quad (131)$$

If we substitute

$$\alpha = k_p u[M] \quad (132a)$$

$$\beta = k'_p \quad (132b)$$

$$\gamma = k_p[M] + k'_p + k_{tr,M}[M] + k_{tr,S}[S] + k_t[P] \quad (132c)$$

$$\theta = k_{tr,M}[M] + k_{tr,S}[S] + k_t[P] \quad (132d)$$

Eq. 125 reduces to the set of algebraic equations given in Eq. A1 in the appendix. Then in terms of  $P_1$ ,  $P_n$  can be determined as

$$[P_n] = [P_1](\alpha x_\infty)^{n-1} \quad (133)$$

But

$$[P] = \sum_{n=1}^{\infty} [P_n] = [P_1]\{1 + \alpha x_\infty + (\alpha x_\infty)^2 + \dots\} = \frac{[P_1]}{(1 - \alpha x_\infty)}$$

or

$$[P_1] = (1 - \alpha x_\infty)[P] \quad (134)$$

Equation 133 therefore reduces to

$$[P_n] = [P](1 - \alpha x_\infty)(\alpha x_\infty)^{n-1} \quad (135)$$

The mole balance of inactive polymer  $M_n$  is given by

$$\frac{d[M_n]}{dt} = \{k_{tr,M}[M] + k_{tr,S}[S] + k_{td}[P]\}[P_n] + \frac{k_{tc}}{2} \sum_{r=1}^{n-1} [P_r][P_{n-r}] \quad (136)$$

One defines the following  $k$ th moment of  $M_n$  distributions as

$$\lambda_k = \sum_{n=1}^{\infty} n^k [M_n] \quad (137)$$

and the moment generation relations for  $\lambda_0$ ,  $\lambda_1$ , and  $\lambda_2$  can be easily derived as

$$\frac{d\lambda_0}{dt} = \{k_{tr,S}[S] + k_{tr,M}[M] + k_{td}[P]\}(1 - \alpha x_\infty)[P] \frac{\alpha x_\infty}{1 - \alpha x_\infty} + \frac{1}{2} k_{tc}[P]^2 \quad (138a)$$

$$\frac{d\lambda_1}{dt} = \{k_{tr,S}[S] + k_{tr,M}[M] + k_{tc}[P]^2\} \frac{1}{1 - \alpha x_\infty}$$

$$\frac{d\lambda_2}{dt} = \{k_{tr,S}[S] + k_{tr,M}[M] + k_{tc}[P]^2\} \frac{1}{1 - \alpha x_\infty}$$

Equations 138 reveal that the polymerization are a function of the constant. Irreversible polymerization compared with Eqs. 138, it is seen in these equations defined as

$$\alpha^* = \frac{k_p u[M]}{k_p[M] + k_{tr,S}[S] + k_t[P]}$$

It can be shown that as  $k'_p \rightarrow 0$ , the most general form of the results

## CONCLUSIONS

Polymerization can in general be divided into two categories: step growth polymerization and chain growth polymerization. In any reasonable model, the number of sites on a  $P_r$  monomer is either branched or linear. In any reasonable model, the number of sites on a  $P_r$  monomer is either branched or linear.

Step growth polymerization involves the reaction of bifunctional monomers has been used to describe the MWD equations can be derived. The reversible polymerization involves the reaction of branched monomers has been used to describe the MWD equations can be derived. Numerical solution of the MWD equations can be derived. Numerical solution of the MWD equations can be derived.

Chain growth polymerization involves the reaction of monomers has been used to describe the MWD equations can be derived. Numerical solution of the MWD equations can be derived. Numerical solution of the MWD equations can be derived.



$$\frac{d\lambda_1}{dt} = \{k_{tr,S}[S] + k_{tr,M}[M] + k_{td}[P]\}[P_1] \frac{(\alpha x_\infty)(2 - \alpha x_\infty)}{(1 - \alpha x_\infty)^2} + \frac{k_{tc}[P_1]^2}{(1 - \alpha x_\infty)^3} \quad (138b)$$

$$\frac{d\lambda_2}{dt} = \{k_{tr,S}[S] + k_{tr,M}[M] + k_{td}[P]\}[P_1] \frac{4(\alpha x_\infty) - 3(\alpha x_\infty)^2 + (\alpha x_\infty)^3}{(1 - \alpha x_\infty)^3} + k_{tc}[P_1]^2 \frac{2 + \alpha x_\infty}{(1 - \alpha x_\infty)^4} \quad (138c)$$

Equations 138 reveal that the moments of the polymer formed by reversible radical polymerization are a function of a term  $(\alpha x_\infty)$  in which  $x_\infty$  involves the reverse rate constant. Irreversible polymerization has been completely analyzed in the literature. On comparison with Eqs. 138, it is found that irreversible polymerization has a form identical to that seen in these equations if  $(\alpha x_\infty)$  is replaced by probability of propagation,  $\alpha^*$ , defined as

$$\alpha^* = \frac{k_p[M]}{k_p[M] + k_{tr,S}[S] + k_{tr,M}[M] + k_t[P]} \quad (139)$$

It can be shown that as  $k'_p \rightarrow 0$ ,  $(\alpha x_\infty)$  reduces to  $\alpha^*$  and in this regard Eqs. 138 give the most general form of the result.

## CONCLUSIONS

Polymerization can in general be classified as step growth and chain growth type. In this chapter it is observed that polymer formation, like any other reaction in nature, is reversible. In any reasonable modeling, this must be taken into account.

Step growth polymerization of bifunctional monomers leads to the formation of linear chains, whereas for that of monomers having functionality more than 2, the resultant polymer is either branched or network. The reversible step growth polymerization of bifunctional monomers has been modeled and it is shown that under a certain transformation, the MWD equations can be decoupled and are considerably easier to solve numerically. The reversible polymerization of multifunctional monomers can be modeled only after the reaction of branched molecules is written. In order to do that, one needs to know the number of sites on a  $P_r$  molecule which would give  $P_n$  ( $n < r$ ) on cleavage. This has been denoted by  $\delta_{r \rightarrow n}$  and it is shown that the MWD equations for reversible multifunctional polymerization involves this factor.  $\delta_{r \rightarrow n}$  is dependent on the chain structure, and there is a computer program that gives the value for specified chain length and structure. Numerical solution of the MWD shows that the polydispersity index of the polymer formed is higher than that of the polymer formed through irreversible mechanism.

Chain growth polymerization can occur through an ionic as well as a radical mechanism, and the discussion is focused on the latter in view of its industrial importance. It is shown that radical polymerization involves three steps: initiation, propagation, and termination. If the polymerization is carried out at low temperatures, the polymerization is essentially irreversible and can be roughly divided into initial and advanced stages which are separated by a gel point. Beyond the gel point the termination rate constants become diffusion controlled and there is a considerable drop in magnitude, which gives a very high rate of polymerization with a corresponding increase in the average chain length of the polymer. The overall polymerization at low temperatures is not limited by the equilibrium but by the occurrence of a glass state of the reaction mass. To control molecular

weight in radical polymerization, one is forced to use high temperatures to suppress the formation of the undesirable glassy state, but some of the reaction steps then become reversible. A kinetic scheme for radical polymerization has been discussed and analyzed for the average chain length and the polydispersity index of polymerization.

## APPENDIX: ANALYTICAL SOLUTION OF ALGEBRAIC EQUATIONS INVOLVED IN ADDITION POLYMERIZATION

Let us consider the following infinite set of algebraic equations which must be solved for  $p_n$  for all  $n$ :

$$\begin{aligned} \frac{p_2}{\theta} &= \frac{p_{20}}{\theta} + \alpha(p_1 - p_2) + \beta(p_3 - p_2) \\ \frac{p_3}{\theta} &= \frac{p_{30}}{\theta} + \alpha(p_2 - p_3) + \beta(p_4 - p_3) \\ &\vdots \\ \frac{p_n}{\theta} &= \frac{p_{n0}}{\theta} + (p_{n-1} - p_n) + (p_{n+1} - p_n) \end{aligned} \quad (A1)$$

where  $p_{i0}$  (for  $i = 1, 2, 3, \dots$ ),  $\alpha$ ,  $\theta$ , and  $\beta$  are constants.

In order to solve for  $p_n$  for all  $n$ , it is assumed that  $p_{N_1+1}$  is known precisely, where  $N_1$  is any integer greater than 2. Equation A1 yields  $p_{N_1}$  as

$$p_{N_1} = x_{N_1} p_{N_1-1} + y_{N_1} p_{N_1} + \frac{1}{\theta} Z_{N_1 N_1} p_{N_{10}} \quad (A2)$$

where

$$x_{N_1} = \frac{1}{\gamma} \quad (A3a)$$

$$y_{N_1} = \frac{1}{\gamma} \quad (A3b)$$

$$Z_{N_1 N_1} = \frac{1}{\gamma} \quad (A3c)$$

$$\gamma = \left( \alpha + \beta + \frac{1}{\theta} \right) \quad (A3d)$$

The expression for  $p_{N_1-1}$  involves  $p_{N_1}$ , which can be eliminated using Eq. A2. This way  $p_{N_1-1}$  can be written in terms of  $p_{N_1-2}$  and  $p_{N_1+1}$ . Proceeding in this way, it is possible to derive for any  $n$  ( $n < N_1$ )

$$p_n = \alpha x_n p_{n-1} + \beta y_n p_{N_1+1} + \frac{1}{\theta} \sum_{i=n}^{N_1} Z_{in} p_{i0} \quad (A4)$$

where

$$x_n = \frac{1}{\gamma - \alpha \beta x_{n+1}} \quad (A5a)$$

$$y_n = \frac{\beta y_{n+1}}{\gamma - \alpha \beta x_{n+1}} =$$

$$Z_{in} = \begin{cases} x_n \\ \frac{\gamma}{\beta} y_{N_1+n-i} \\ y_n \end{cases}$$

Proceeding this way, it is p

We next examine the pr  
Eq. A5a can be written in t

$$\lim_{N_1 \rightarrow \infty} x_n \triangleq x_\infty = \frac{1}{\gamma - \frac{1}{\gamma - x_\infty}}$$

$$n \ll N_1$$

As  $N_1 \rightarrow \infty$ ,  $x_n$  for  $n \ll N_1$  a  
gives

$$x_\infty = \frac{1}{\gamma - \frac{1}{\gamma - x_\infty}}$$

where

$$\gamma_1 = \frac{\gamma}{\alpha \beta}$$

Equation A7 can be solved fo

$$x_\infty = \frac{\gamma - \sqrt{\gamma^2 - 4\alpha\beta}}{2\alpha\beta}$$

where the lower root serves a

To study the properties of  
first recognized that no matte  
unity:

$$\begin{aligned} \beta x_\infty &= \beta \frac{\gamma}{2\alpha\beta} \left\{ 1 - \sqrt{1 - \frac{4\alpha\beta}{\gamma^2}} \right\} \\ &= \left( \frac{\gamma}{2\alpha} \right) \left\{ \frac{1}{2} \frac{2\alpha}{\gamma} \frac{2\beta}{\gamma} + \right. \end{aligned}$$

i.e., since  $\alpha/\gamma$  and  $\beta/\gamma$  both a  
recalled from Eq. A5 that  $y_n =$   
 $x_n = x_\infty$  is a good approximati

$$y_{n-i} = y_n^* (\beta x_\infty)^i, \quad i = 1, 2, \dots$$

Since  $(\beta x_\infty) < 1$ ,  $y_n$  can be m  
large. Furthermore, as  $N_1 \rightarrow \infty$

gh temperatures to suppress the the reaction steps then become has been discussed and analyzed of polymerization.

## ALGEBRAIC EQUATIONS

ations which must be solved for

$$y_n = \frac{\beta y_{n+1}}{\gamma - \alpha \beta x_{n+1}} = \frac{1}{\beta} \prod_{i=n}^{N_1} (\beta x_i), \quad 2 \leq n \leq N \quad (\text{A5b})$$

$$Z_{in} = \begin{cases} x_n & \text{for } i = n \\ \frac{\gamma}{\beta} y_{N_1+n-i} & \text{for } n+1 \leq i \leq N_1-1 \\ y_n & \text{for } i = N_1 \end{cases} \quad (\text{A5c})$$

Proceeding this way, it is possible to determine  $p_1$  in terms of  $p_{N_1+1}$ .

We next examine the properties of the solution as  $N_1$  approaches  $\infty$ . The value of  $x_n$  in Eq. A5a can be written in the form of an infinite successive fraction as

$$\lim_{N_1 \rightarrow \infty} x_n \triangleq x_\infty = \frac{1}{\gamma - \frac{\alpha \beta}{\gamma - \frac{\alpha \beta}{\gamma - \frac{\alpha \beta}{\gamma - \dots}}}} \quad (\text{A6})$$

As  $N_1 \rightarrow \infty$ ,  $x_n$  for  $n \ll N_1$  approaches an asymptotic value independent of  $n$ , and Eq. A6 gives

$$x_\infty = \frac{1}{\gamma - \frac{1}{\gamma_1 - x_\infty}} \quad (\text{A7})$$

where

$$\gamma_1 = \frac{\gamma}{\alpha \beta} \quad (\text{A8})$$

Equation A7 can be solved for  $x_\infty$  as

$$x_\infty = \frac{\gamma - \sqrt{\gamma^2 - 4\alpha\beta}}{2\alpha\beta} \quad (\text{A9})$$

where the lower root serves as a physically relevant quantity.

To study the properties of the infinite continued fraction formed by  $y_n$  in Eq. A5, it is first recognized that no matter what the values of  $\alpha$ ,  $\beta$ , and  $\theta$ ,  $\beta x_\infty$  is always less than unity:

$$\begin{aligned} \beta x_\infty &= \beta \frac{\gamma}{2\alpha\beta} \left\{ 1 - \sqrt{1 - \frac{2\alpha}{\gamma} \frac{2\beta}{\gamma}} \right\} \\ &= \left( \frac{\gamma}{2\alpha} \right) \left\{ \frac{1}{2} \frac{2\alpha}{\gamma} \frac{2\beta}{\gamma} + o\left( \frac{\alpha^2}{\gamma^2} \frac{\beta^2}{\gamma^2} \right) \right\} = \frac{\beta}{\gamma} + o\left( \frac{\alpha^2}{\gamma^2} \frac{\beta^2}{\gamma^2} \right) \end{aligned} \quad (\text{A10})$$

i.e., since  $\alpha/\gamma$  and  $\beta/\gamma$  both are less than unity,  $(\beta x_\infty)$  is always less than unity. If it is recalled from Eq. A5 that  $y_n = y_{n+1}(\beta x_\infty)$  and if we denote by  $y_n^*$  the value of  $n$  at which  $x_n = x_\infty$  is a good approximation, then  $y_{n-1}$ ,  $y_{n-2}$ , etc., can be written as

$$y_{n-i} = y_n^* (\beta x_\infty)^i, \quad i = 1, 2, \dots, n-1 \quad (\text{A11})$$

Since  $(\beta x_\infty) < 1$ ,  $y_n$  can be made sufficiently close to zero by choosing  $N_1$  sufficiently large. Furthermore, as  $N_1 \rightarrow \infty$  and  $n \ll N_1$ , the following are also true:

$$Z_n \rightarrow x_\infty \quad (\text{A12a})$$

$$Z_{N_1 n} \rightarrow 0 \quad (\text{A12b})$$

or more generally

$$Z_{in} \rightarrow x_\infty (\beta x_\infty)^{i-n}, \quad \text{for } n \leq i \quad (\text{A13})$$

As  $N_1 \rightarrow \infty$ ,  $p_n$  in Eq. A1 is given by

$$p_n = \frac{x}{\theta} \sum_{i=n}^{\infty} (\beta x_\infty)^{i-n} p_{i0} + (\alpha x_\infty) p_{n-1} \quad (\text{A14})$$

and this gives  $p_n$  for all  $n$  in Eq. A1 as follows. Using this,  $p_2$  is written in terms of  $p_1$ , which is substituted in the relation of  $p_1$ , and  $p_n$  is determined by successively evaluating  $p_2, p_3$ , etc.

## REFERENCES

1. P. J. Flory, *Principles of Polymer Chemistry*, Cornell University Press, Ithaca, N.Y. (1953).
2. R. W. Lenz, *Organic Chemistry of Synthetic High Polymers*, Wiley, New York (1967).
3. A. Kumar and S. K. Gupta, *Fundamentals of Polymer Science and Engineering*, Tata McGraw-Hill, New Delhi (1978).
4. P. E. M. Allen and C. R. Patrick, *Kinetics and Mechanism of Polymerization Reactions*, Ellis Horwood, Chichester (1974).
5. J. Furukawa and O. Vogl, *Ionic Polymerization, Unsolved Problems*, Marcel Dekker, New York (1976).
6. T. Keii, *Kinetics of Ziegler-Natta Polymerization*, Kodansha, Tokyo (1972).
7. J. Boor, *Ziegler-Natta Catalysts and Polymerizations*, Academic Press, New York (1979).
8. J. C. W. Chien, *Coordination Polymerization*, Academic Press, New York (1975).
9. G. Odian, *Principles of Polymerization*, 2nd ed., Wiley, New York (1981).
10. A. Kumar, *J. Appl. Polym. Sci.*, **34**: 571 (1987).
11. S. K. Gupta, A. Kumar, and K. K. Agarwal, *J. Appl. Polym. Sci.*, **27**: 3089 (1982).
12. K. Tai, Y. Arai, H. Teranishi, and T. Tagawa, *J. Appl. Polym. Sci.*, **25**: 1789 (1980).
13. S. K. Gupta and A. Kumar, *Chem. Eng. Comm.*, **20**: 1 (1983).
14. H. Kilson, *Ind. Eng. Chem. Fundam.*, **7**: 354 (1968).
15. J. A. Biesenberger, *AIChEJ*, **11**: 369 (1965).
16. A. Kumar, P. Rajora, N. L. Agarwalla, and S. K. Gupta, *Polymer*, **23**: 222 (1982).
17. H. M. Hulbert and S. Katz, *Chem. Eng. Sci.*, **19**: 555 (1964).
18. A. Kumar, *Macromolecules*, **20**: 220 (1987).
19. A. Kumar, S. N. Sharma, and S. K. Gupta, *J. Appl. Polym. Sci.*, **29**: 1045 (1984).
20. A. Kumar, S. N. Sharma, and S. K. Gupta, *Polym. Eng. Sci.*, **24**: 1205 (1984).
21. A. Kumar, S. K. Gupta, and D. Kunzru, *J. Appl. Polym. Sci.*, **27**: 4421 (1982).
22. D. H. Solomon, ed., *Step Growth Polymerization*, Marcel Dekker, New York (1972).
23. M. Amon and C. D. Denson, *Ind. Eng. Chem. Fundam.*, **19**: 415 (1980).
24. S. K. Gupta, N. L. Agarwalla, and A. Kumar, *J. Appl. Polym. Sci.*, **27**: 1217 (1982).
25. S. K. Gupta, A. Kumar, and K. K. Agarwal, *Polymer*, **23**: 1367 (1982).
26. L. C. Case, *J. Polym. Sci.*, **29**: 455 (1958).
27. V. S. Nanda and S. C. Jain, *J. Chem. Phys.*, **49**: 1318 (1968).
28. G. B. Taylor, *J. Am. Chem. Soc.*, **69**: 638 (1947).
29. S. I. Kuchanov, M. L. Keshtov, P. G. Halatur, V. A. Vasnev, S. V. Vinogradova, and V. V. Korshak, *Macromol. Chem.*, **184**: 105 (1983).
30. S. K. Gupta, N. L. Agarwalla, P. Rajora, and A. Kumar, *J. Polym. Sci. Polym. Phys. Ed.*, **20**: 933 (1982).
31. R. Goel, S. K. Gupta, and A. Kumar, *J. Polym. Sci. Polym. Phys. Ed.*, **20**: 933 (1982).
32. S. K. Gupta, A. Kumar, and A. Kumar, *J. Polym. Sci. Polym. Phys. Ed.*, **20**: 933 (1982).
33. S. K. Gupta, A. Kumar, and A. Kumar, *J. Polym. Sci. Polym. Phys. Ed.*, **20**: 933 (1982).
34. A. Kumar, S. K. Gupta, and A. Kumar, *J. Polym. Sci. Polym. Phys. Ed.*, **20**: 933 (1982).
35. S. K. Gupta, A. Kumar, and A. Kumar, *J. Polym. Sci. Polym. Phys. Ed.*, **20**: 933 (1982).
36. A. S. Gupta, A. Kumar, and A. Kumar, *J. Polym. Sci. Polym. Phys. Ed.*, **20**: 933 (1982).
37. R. W. Lenz, C. E. Hanlov, and A. Kumar, *J. Polym. Sci. Polym. Phys. Ed.*, **20**: 933 (1982).
38. J. H. Hodkin, *J. Polym. Sci. Polym. Phys. Ed.*, **20**: 933 (1982).
39. P. J. Flory, *J. Am. Chem. Soc.*, **77**: 3701 (1955).
40. P. J. Flory, *Chem. Rev.*, **39**: 1 (1959).
41. W. H. Stockmayer, *J. Chem. Phys.*, **17**: 127 (1949).
42. W. H. Stockmayer, *J. Chem. Phys.*, **18**: 108 (1950).
43. W. H. Stockmayer, *J. Polym. Sci.*, **3**: 102 (1948).
44. W. H. Stockmayer, *J. Polym. Sci.*, **3**: 102 (1948).
45. M. Gordon, *Proc. R. Soc. London*, **A263**: 1 (1960).
46. D. S. Hutler, G. N. Malcol, and A. Kumar, *J. Polym. Sci. Polym. Phys. Ed.*, **20**: 933 (1982).
47. M. Gordon and T. G. Parke, *J. Polym. Sci. Polym. Phys. Ed.*, **20**: 933 (1982).
48. M. Gordon, T. C. Ward, and A. Kumar, *J. Polym. Sci. Polym. Phys. Ed.*, **20**: 933 (1982).
49. M. Gordon and G. R. Scant, *J. Polym. Sci. Polym. Phys. Ed.*, **20**: 933 (1982).
50. M. Gordon and M. Judd, *Nature*, **163**: 694 (1949).
51. K. Dusek, M. Gordon, and A. Kumar, *J. Polym. Sci. Polym. Phys. Ed.*, **20**: 933 (1982).
52. T. E. Harris, *Theory of Branched Polymers*, Academic Press, New York (1954).
53. C. W. Macosko and D. R. Miller, *J. Polym. Sci. Polym. Phys. Ed.*, **20**: 933 (1982).
54. D. R. Miller and C. W. Macosko, *J. Polym. Sci. Polym. Phys. Ed.*, **20**: 933 (1982).
55. D. R. Miller and C. W. Macosko, *J. Polym. Sci. Polym. Phys. Ed.*, **20**: 933 (1982).
56. D. R. Miller, E. M. Valles, and A. Kumar, *J. Polym. Sci. Polym. Phys. Ed.*, **20**: 933 (1982).
57. D. R. Miller and C. W. Macosko, *J. Polym. Sci. Polym. Phys. Ed.*, **20**: 933 (1982).
58. R. F. T. Stepto, in *Developments in Polymer Science*, Interscience Publishers, Barking, England (1965).
59. J. L. Stanford and R. F. T. Stepto, *Polymer*, **20**: 1045 (1979).
60. R. F. T. Stepto, *Polymer*, **20**: 1045 (1979).
61. A. B. Fasina and R. F. T. Stepto, *Polymer*, **20**: 1045 (1979).
62. K. Dusek and W. Prins, *Adv. Chem. Ser.*, **122**: 1 (1974).
63. W. B. Temple, *Makromol. Chem.*, **122**: 1 (1974).
64. H. Jacobson and W. H. Stockmayer, *J. Chem. Phys.*, **18**: 16 (1950).
65. M. Gordon and W. B. Temple, *J. Polym. Sci. Polym. Phys. Ed.*, **20**: 933 (1982).
66. N. A. Plate and O. V. Noah, *Vysokomol. Soedin. A*, **1**: 1 (1959).
67. I. I. Romanstova, Yu. A. Tarasov, and N. A. Plate, *Vysokomol. Soedin. A*, **1**: 1 (1959).
68. S. K. Gupta, S. Nath, and A. Kumar, *J. Polym. Sci. Polym. Phys. Ed.*, **20**: 933 (1982).
69. M. Abramowitz and J. A. Stegun, *Handbook of Mathematical Functions*, NBS Monograph 9, U.S. Government Printing Office, Washington, D.C. (1965).
70. A. Kumar and S. K. Gupta, *J. Polym. Sci. Polym. Phys. Ed.*, **20**: 933 (1982).
71. M. Mutter, U. W. Suter, and P. J. Flory, *J. Polym. Sci. Polym. Phys. Ed.*, **20**: 933 (1982).
72. A. Kumar and P. K. Khandehval, *J. Polym. Sci. Polym. Phys. Ed.*, **20**: 933 (1982).
73. A. Kumar and P. K. Khandehval, *J. Polym. Sci. Polym. Phys. Ed.*, **20**: 933 (1982).
74. A. Kumar and P. K. Khandehval, *J. Polym. Sci. Polym. Phys. Ed.*, **20**: 933 (1982).
75. R. W. Lenz, *Organic Chemistry of Polymers*, Wiley, New York (1975).
76. J. Brandrup and E. H. Immergut, *Polymer Handbook*, Wiley, New York (1975).

- (A12a) 31. R. Goel, S. K. Gupta, and A. Kumar, *Polymer*, 18: 851 (1977).
- (A12b) 32. S. K. Gupta, A. Kumar, and A. Bhargava, *Eur. Polym. J.*, 15: 557 (1979).
33. S. K. Gupta, A. Kumar, and A. Bhargava, *Polymer*, 20: 305 (1979).
34. A. Kumar, S. K. Gupta, and R. Saraf, *Polymer*, 21: 1323 (1980).
- (A13) 35. S. K. Gupta, A. Kumar, and R. Saraf, *J. Appl. Polym. Sci.*, 25: 1049 (1980).
36. A. S. Gupta, A. Kumar, and S. K. Gupta, *Br. Polym. J.*, 13: 76 (1981).
37. R. W. Lenz, C. E. Hanlovitz, and H. A. Smith, *J. Polym. Sci.*, 58: 351 (1962).
38. J. H. Hodkin, *J. Polym. Sci. Polym. Chem. Ed.*, 14: 409 (1976).
- (A14) 39. P. J. Flory, *J. Am. Chem. Soc.*, 63: 3083 (1941).
40. P. J. Flory, *Chem. Rev.*, 39: 137 (1949).
41. W. H. Stockmayer, *J. Chem. Phys.*, 11: 45 (1943).
42. W. H. Stockmayer, *J. Chem. Phys.*, 12: 125 (1944).
43. W. H. Stockmayer, *J. Polym. Sci.*, 9: 69 (1952).
44. W. H. Stockmayer, *J. Polym. Sci.*, 11: 424 (1953).
45. M. Gordon, *Proc. R. Soc. London A*, 268: 240 (1962).
46. D. S. Hutler, G. N. Malcolm, and M. Gordon, *Proc. R. Soc. London A*, 295: 29 (1966).
47. M. Gordon and T. G. Parker, *Proc. R. Soc. Edinburgh*, A69: 181 (1970).
48. M. Gordon, T. C. Ward, and R. S. Whitney, in *Polymer Networks* (A. J. Chompt and S. Newman, eds.), Plenum, New York, pp. 1-21 (1971).
49. M. Gordon and G. R. Scantlebury, *J. Chem. Soc. London B*, 1 (1967).
50. M. Gordon and M. Judd, *Nature*, 234: 96 (1971).
51. K. Dusek, M. Gordon, and S. B. Ross-Murphy, *Macromolecules*, 11: 236 (1978).
52. T. E. Harris, *Theory of Branching Processes*, Springer-Verlag, Berlin, Chap. 1 (1963).
53. C. W. Macosko and D. R. Miller, *Macromolecules*, 9: 199 (1976).
54. D. R. Miller and C. W. Macosko, *Macromolecules*, 9: 206 (1976).
55. D. R. Miller and C. W. Macosko, *Macromolecules*, 11: 656 (1978).
56. D. R. Miller, E. M. Valles, and C. W. Macosko, *Polym. Eng. Sci.*, 19: 272 (1979).
57. D. R. Miller and C. W. Macosko, *Macromolecules*, 13: 1063 (1980).
58. R. F. T. Stepto, in *Developments in Polymerization*, Vol. 3 (R. N. Haward, ed.), Applied Science Publishers, Barking, U.K., p. 81 (1982).
59. J. L. Stanford and R. F. T. Stepto, *Br. Polym. J.*, 9: 124 (1977).
60. R. F. T. Stepto, *Polymer*, 20: 1324 (1979).
61. A. B. Fasina and R. F. T. Stepto, *Makromol. Chem.*, 182: 2479 (1981).
62. K. Dusek and W. Prins, *Adv. Polym. Sci.*, 6: 1 (1969).
63. W. B. Temple, *Makromol. Chem.*, 160: 277 (1972).
64. H. Jacobson and W. H. Stockmayer, *J. Chem. Phys.*, 18: 1600 (1950).
65. M. Gordon and W. B. Temple, *Makromol. Chem.*, 263 (1972).
66. N. A. Plate and O. V. Noah, *Adv. Polym. Sci.*, 31: 133 (1979).
67. I. I. Romanstova, Yu. A. Taran, O. V. Noa, A. M. Yelyashevich, Yu. Ya. Gotlib, and N. A. Plate, *Vysokomol. Soedin. A*, 19: 2800 (1977).
68. S. K. Gupta, S. Nath, and A. Kumar, *J. Appl. Polym. Sci.*, 30: 557 (1985).
69. M. Abramowitz and J. A. Stegun, *Handbook of Mathematical Functions*, Dover, New York (1965).
70. A. Kumar and S. K. Gupta, *J. Macromol. Sci., Rev. Chem. Phys.*, C26: 183 (1986).
71. M. Mutter, U. W. Suter, and P. J. Flory, *J. Am. Chem. Soc.*, 98: 5745 (1976).
72. A. Kumar and P. K. Khandelwal, *J. Appl. Polym. Sci.*, 33: 1835 (1987).
73. A. Kumar and P. K. Khandelwal, *Polym. Commun.*, 28: 48 (1987).
74. A. Kumar and P. K. Khandelwal, *Modelling of Reversible Multifunctional Step Growth Polymerization*, M. Tech. Thesis, 11 T Kanpur, India, 1986.
75. R. W. Lenz, *Organic Chemistry of Synthetic High Polymers*, Interscience, New York (1967).
76. J. Brandrup and E. H. Immergent, *Polymer Handbook*, 2nd ed., Wiley-Interscience, New York (1975).

77. G. Odian, *Principles of Polymerization*, 2nd ed., McGraw-Hill, New York (1982).
78. O. Levenspiel, *Chemical Reaction Engineering*, 2nd ed., Wiley, New York (1972).
79. W. H. Ray, On the Mathematical Modelling of Polymerization Reactors, *J. Macromol. Sci. Rev. Macromol. Chem.*, C8: 1 (1973).
80. S. L. Liu and N. R. Amundson, *Rubber Chem. Tech.*, 34: 995 (1961).
81. P. G. Gladyshev and S. R. Ratikov, *Russ. Chem. Rev.*, 35: 405 (1966).
82. J. Cardenas and K. F. O'Driscoll, *J. Polym. Sci. Polym. Chem. Ed.*, 14: 883 (1976).
83. F. L. Marten and A. E. Hamielec, *ACS Symp. Ser.*, 104 (1979).
84. S. K. Soh and D. C. Sundberg, *J. Polym. Sci. Polym. Chem. Ed.*, 20: 1299 (1982).
85. S. K. Soh and D. C. Sundberg, *J. Polym. Sci. Polym. Chem. Ed.*, 20: 1315 (1982).
86. S. K. Soh and D. C. Sundberg, *J. Polym. Sci. Polym. Chem. Ed.*, 20: 1331 (1982).
87. S. K. Soh and D. C. Sundberg, *J. Polym. Sci. Polym. Chem. Ed.*, 20: 1345 (1982).
88. W. Y. Chiu, G. M. Carratt, and D. S. Soong, 16: 348 (1983).
89. T. J. Tulig and M. Tirrell, *Macromolecules*, 14: 1501 (1981).
90. D. T. Turner, *Macromolecules*, 10: 221 (1977).
91. J. Cardenas and K. F. O'Driscoll, *J. Polym. Sci. Polym. Chem. Ed.*, 15: 1883 (1977).
92. J. Cardenas and K. F. O'Driscoll, *J. Polym. Sci. Polym. Chem. Ed.*, 15: 2097 (1977).
93. K. F. O'Driscoll, J. M. Dionisio, and H. K. Mahabadi, in *Polymerization Reactors and Processes* (J. N. Henderson and T. C. Bouton, eds.), American Chemical Society, Washington (1979).
94. F. L. Marten and A. E. Hamielec, *J. Appl. Polym. Sci.*, 27: 489 (1982).
95. T. J. Tulig and M. Tirrell, *Macromolecules*, 15: 459 (1981).

## Optimizat

### INTRODUCTION

#### SOME ASPECTS OF OPTIMIZ

Polymerization Kinetics and

Reactor Dynamics and Stabili

Mathematical Tools of Optim

#### FORMULATION OF THE OBJ

The Multiobjective Nature of

Multiobjective Decision Anal

#### OVERVIEW OF PREVIOUS CO

#### BATCH CHAIN POLYMERIZA

The Minimum Time Problem

Modification of Molecular We

#### STEP REACTIONS

#### COPOLYMERIZATION REACT

#### OPTIMIZATION OF TRANSIEN

#### CONCLUSION

#### NOTATION

#### REFERENCES

### INTRODUCTION

The relevance of optimization are easily justified by the econ The manufacture of polymeric volume of chemical production support of optimization are fo polymeric material cannot be co tion by itself does not determi related to the applicability, qua properties, like processability a molecular weight distribution (M

\*Current affiliation: Tremco Ltd., Toro

1'1  
6861  
9E4'  
88E

ISBN 0-8247-8173-2

Copyright © 1989 by MARCEL DEKKER, INC. All Rights Reserved

Neither this book nor any part may be reproduced or transmitted in any form or by any means, electronic or mechanical, including photocopying, microfilming, and recording, or by any information storage and retrieval system, without permission in writing from the publisher.

the publisher.

MARCEL DEKKER, INC.  
270 Madison Avenue, New York, New York 10016

Current printing (last digit):

10 9 8 7 6 5 4 3 2 1

PRINTED IN THE UNITED STATES OF AMERICA

*The Handbook of Polymer Chemistry*, Volume 1, *Synthetic Polymer Chemistry*. This first volume of the series presents the efforts of twenty-five researchers, all of whom sent the work embodies the statements, recommendations, and performance properties. The data derived are essentially cross-referenced and organized into twelve chapters. Included in this production of these various technical techniques for characterization of the principles behind the data derived are essential performance properties. This first volume of the series presents the efforts of twenty-five researchers, all of whom sent the work embodies the statements, recommendations, and performance properties. The data derived are essentially cross-referenced and organized into twelve chapters. Included in this production of these various technical techniques for characterization of the principles behind the data derived are essential performance properties.

---

# Handbook of Polymer Science and Technology

---

Volume 1  
Synthesis and Properties

---

Edited by: Nicholas P. Cheremisinoff